Water at Interfaces

Olle Björneholm[1], Martin H. Hansen[2,7], Andrew Hodgson[3], Li-Min Liu[4,5], David T. Limmer[6], Angelos Michaelides[4], Philipp Pedevilla[4], Jan Rossmeisl[7], Huaze Shen[8], Gabriele Tocci[4], Eric Tyrode[9], Marie-Madeleine Walz[1,#] , Josephina Werner[1,10], Hendrik Bluhm[11,*]

[1]*Department of Physics and Astronomy, Uppsala University, SE 75105 Uppsala, Sweden*

[2]*Technical University of Denmark, 2800 Kongens Lyngby, Denmark.*

[3]*Department of Chemistry, University of Liverpool, Liverpool L69 7ZD, United Kingdom.*

[4]*Thomas Young Centre, London Centre for Nanotechnology, and Department of Chemistry, University College London, London WC1E 6BT, United Kingdom.*

[5]*Beijing Computational Science Research Center, Beijing, 100193, China.*

[6]*Princeton Center for Theoretical Science, Princeton University, Princeton, USA.*

[7]*Department of Chemistry, University of Copenhagen, Universitetsparken 5, 2100 Copehagen.*

[8]*International Center for Quantum Materials and School of Physics, Peking University, Beijing 100871, China.*

[9]*Department of Chemistry, KTH Royal Institute of Technology, 10044 Stockholm, Sweden.10*

[10] *Department of Chemistry and Biotechnology, Swedish University of Agricultural Sciences, Box 7015, SE-750 07 Uppsala, Sweden.*

[11]*Chemical Sciences Division, Lawrence Berkeley National Laboratory, Berkeley, CA 94720, USA.*

 # present address: Department of Cell and Molecular Biology, Uppsala University, Box 596, SE-751 24 Uppsala, Sweden.

CONTENTS

ABSTRACT

The interfaces of neat water and aqueous solutions play a prominent role in many technological processes and in the environment. Examples of aqueous interfaces are ultrathin water films that cover most hydrophilic surfaces under ambient relative humidities, the liquid/solid interface which drives many electrochemical reactions, and the liquid/vapor interface, which governs the uptake and release of trace gases by the oceans and cloud droplets. In this article we review some of the recent experimental and theoretical advances in our knowledge of the properties of aqueous interfaces and discuss open questions and gaps in our understanding.

1. INTRODUCTION

Aqueous interfaces are ubiquitous in nature and technology. Processes at aqueous interfaces are paramount to the understanding of the most challenging questions in, e.g., atmospheric science, geochemistry, electrochemistry, and corrosion. For instance, about 50% of CO_2 from anthropogenic sources are taken up by the earth's oceans, where the initial steps of this process happen at the air/ocean interface.[1] Another example are electrochemical reactions, which are controlled by the characteristics of the liquid/solid interface, in particular the properties of the electric double layer.[2] Our knowledge of the fundamental physical chemistry of aqueous interfaces is very limited compared to that of solid surfaces. Although substantial progress has been made over the past decades, the investigation of these interfaces is still a challenge, both using experimental and theoretical methods. One experimental challenges is the high vapor pressure of aqueous solutions at ambient temperatures, which complicates – though no longer prevents – the application of many of the standard surface science techniques that have been successfully used to characterize clean and adsorbate-covered metal, semiconductor, and oxide surfaces. A further

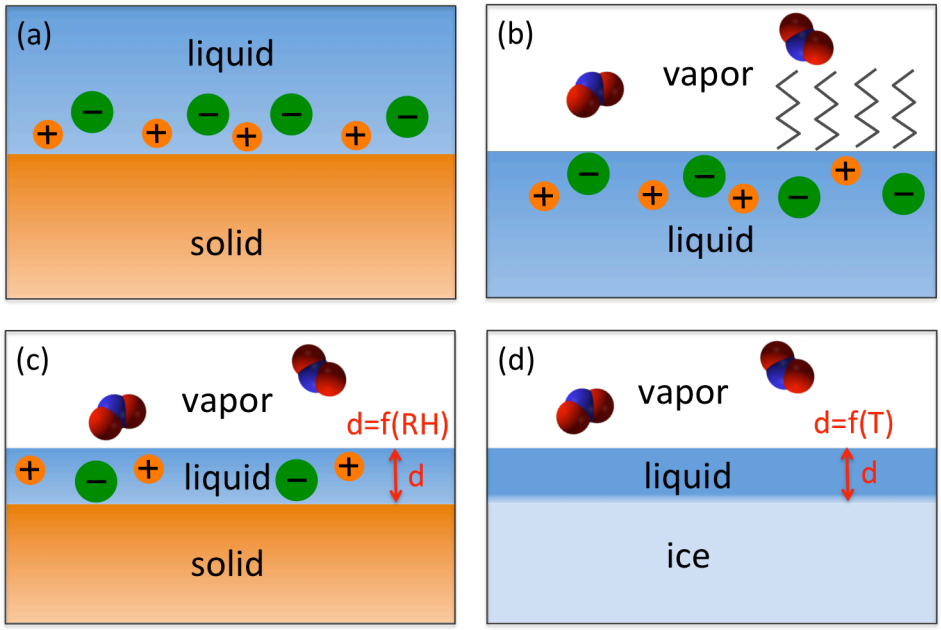

Figure 1. Schematic representation of aqueous interfaces discussed in this review. Examples for **(a)** liquid-solid, **(b)** liquid-vapor, **(c)** thin water films under ambient relative humidity, and **(d)** the liquid-like layer on ice. Although the presence of ions is indicated here, there are a number of model studies on neat water where ions are not present.

complication is the preparation of clean aqueous interfaces under controlled conditions, which is difficult due to the elevated background pressure and limited pumping as well as fast diffusion in liquids that allows trace amounts of bulk contaminants to rapidly accumulate at the interfaces. Theoretical modeling of aqueous solution interfaces is also more challenging compared to that of a solid/adsorbate interfaces due to, e.g., the high fluctuations in the atomic positions in a liquid which requires the sampling of many different configurations, as well as the existing difficulty to adequately describe the intermolecular interactions between water molecules.

The most commonly encountered aqueous interfaces are schematically depicted in Figure 1. The liquid/solid interface (Fig. 1a) plays a crucial role in processes as diverse as photoelectrochemical reactions, the weathering of rocks, and corrosion, and its investigation is arguably the biggest challenge in surface science in the years ahead.[3,4] A detailed understanding of the properties of the liquid/solid interface under *operando* conditions and on the molecular scale is still lacking. A complete investigation of heterogeneous processes at liquid/solid interfaces requires measuring the chemical composition of four distinct regions: (1) The bulk liquid, (2) when present, the electric double layer at the interface, (3) the solid interface in contact with the liquid, and (4) the sub-surface region of the solid. In particular the direct measurement of the chemical species and electric potential distribution across the electric double layer is a major challenge. Experimental measurements of the narrow (a few nanometers wide) interfacial region is complicated by the requirement to enhance the signal from the interface over those of the adjacent bulk liquid and solid phase. The properties of the electric double layer and the near-interface region of the adjacent solid substrate govern mass and charge transport across the interface and thus the rates of, e.g., catalytic reactions and corrosion processes.

Liquid/vapor interfaces (Fig. 1b) play a major role in particular in natural processes. For example, they strongly influence the abundance and reactivity of trace gas molecules that drive heterogeneous processes in atmospheric and environmental chemistry. The chemical composition of the aqueous solution/vapor interface can vary significantly from that of the bulk due to, e.g., differences in the propensity of different ions for the interface, which has direct implications for the modeling of

atmospheric reactions. Surfactants can alter the propensity of the ions for the interface[5] and also strongly influence condensation and evaporation rates.[6] To date, little is known about the concentration of a wide range of solution phase species at the liquid/vapor interface. Even less is known about the fundamental pathways in heterogeneous reactions of gas phase species at liquid/vapor interfaces. Widely-used atmospheric science experimental techniques monitor changes in the gas phase composition to conclude upon reactions at the liquid/vapor interface, but do not provide direct information about the reaction products and other properties of the liquid/vapor interface. However, recent combined non-linear optical spectroscopy, X-ray-absorption and photoemission spectroscopy experiments with molecular dynamics simulations have over the last decade provided new details about the chemical composition of aqueous solution/vapor interfaces as a function of bulk concentration, pH and the presence of surfactants.[7]

Intimately related to the properties of liquid/solid and liquid/vapor interfaces are the initial stages of water reaction with and adsorption on solid substrates, from which with increasing solution film thickness the bulk liquid/solid and liquid/vapor interfaces develop. In the limit of very thin (~nm) solution layers, the liquid/solid and liquid/vapor interfaces interact and jointly determine the properties of the thin solution film (see Fig. 1c). This is the situation for solid surfaces at ambient relative humidity, where – depending on the surface properties of the substrate – a thin water or solution layer is formed, which diverges to a macroscopically thick film (wetting or non-wetting) at the saturation relative humidity. Despite their great importance for, e.g., cloud nucleation and atmospheric corrosion, the initial reaction of water vapor with solid substrates (e.g., hydroxylation vs. water adsorption), the thickness and the structural properties of the thin liquid films as well as their influence on the chemical reactivity and physical properties of the host substrate are largely unexplored.

The last example for an important and ubiquitous aqueous interface is the ice/vapor interface (Fig 1d), which plays a major role in many environmental processes, including thundercloud electrification, frost heave, and heterogeneous chemical reactions in the atmosphere and polar regions. The properties of ice surfaces under environmental and atmospheric conditions, in particular the presence of a liquid-like layer at the ice surface at temperatures close to the melting point, are still far from being understood – indeed,

reported thicknesses of the liquid-like layer at temperatures close to the melting point vary by a factor of up to two orders of magnitude![8] This is partly due to the influence of adsorbates, which most likely influence the onset temperature for pre-melting, and which are difficult to quantify in current experiments. The interaction of trace gases with ice has also attracted considerable attention over the past decades due to its relevance for atmospheric and polar chemistry. Trace gases adsorbed on the ice surface may initiate, e.g., chemical and photochemical processes that are relevant for the ozone layer and the nitrogen oxide budget in the upper troposphere. On Earth, snow covered areas (especially the Arctic) act as sinks and sources for organic and inorganic trace gas species. Systematic investigations are essential that correlate the surface and near-surface chemistry and the properties of the liquid-like layer over the temperature range relevant to atmospheric and environmental science, *i.e.*, >200 K, and relevant trace gas concentrations.

This review briefly summarizes recent progress in these areas and emphasizes existing open questions and challenges to the experimental and theoretical investigation of aqueous interfaces, starting from well-controlled low water coverages on single crystalline metal surfaces at low temperatures and under ultra-high vacuum conditions, to thin water layers under ambient conditions, to the bulk liquid/solid and liquid/vapor interfaces, concluding with the ice/vapor interface. Given the wide variety of aqueous interfaces and the vast number of original publications on this subject, only a subset of topics related to these interfaces are discussed; these topics were chosen for their relevance and also as representatives for a broad range of experimental and theoretical approaches that are being used to gain a deeper understanding of the properties and processes at aqueous interfaces.

2. ULTRATHIN WATER LAYERS AT METAL SURFACES

The application of modern experimental surface science techniques and atomistic computer simulations has made water-metal systems the 'fruit fly' of the water-interfaces field, with detailed studies revealing the atomic structure of water at a number of metal surfaces. As a result we now know rather more about the behavior of water at metal interfaces than at many other surfaces, for example at oxide surfaces, which show more specific chemistry. Here we briefly describe some recent key results that have developed our understanding of the structures formed during water adsorption at low temperatures, before outlining questions still to be resolved. These systems have been reviewed before[9,10,11,12] but the questions we would particularly like to address here include how water bonds to the substrate, the role of water-water versus water-solid bonding, the effect of lattice parameter and symmetry on the water networks formed, what is the molecular orientation of water at the interface, will water form an 'icelike' bilayer, does it dissociate and, finally, how does multilayer formation modify or restructure the interface layer?

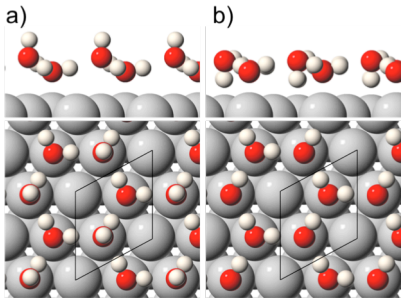

Figure 2. Schematic showing an ordered (√3 x √3)R30° water structure on a close packed surface. a) hypothetical water bilayer with the uncoordinated H atoms on the water either oriented away from the surface ('H-up') or b) in a modified bilayer structure pointing 'H-down' toward the metal.[31]

2.1 Introduction

Water generally adsorbs weakly on transition metal surfaces, with a binding energy similar to that of water on bulk ice. A consequence of this weak interaction is that water is stabilized only by the combination of direct bonding with the metal and hydrogen bonding to other water molecules, allowing us to tune the interface from wetting to non-wetting by varying the metal and surface symmetry. For

example Ag(111) and Cu(111) are hydrophobic and do not wet, whereas Cu(110) and Pt(111) form a stable water layer.[9] The observation of a (√3 x √3)R30° structure on several close packed metal surfaces, and the close match to the lattice spacing of ice, led to the early suggestion that water adopts a simple hexagonal 'icelike' bilayer structure, shown in Figure 2a.[11] This structure has half the water bound atop the metal atoms, via the oxygen atom of water, while the upper layer of water completes the hydrogen bonding network. In this arrangement water occupies a pseudo-tetrahedral environment, with the uncoordinated proton on the upper water molecule pointing away from the metal surface. A similar distorted hexagonal network was proposed for the rectangular f.c.c. (110) surfaces, where a c(2 x 2) structure was found. This model was first challenged in 2002, based on theoretical calculations, when Feibelman suggested that water adsorbed on Ru(0001) should be unstable compared to 3D ice, and that adsorption could be stabilized by partial dissociation to form a mixed OH/water structure.[13] Since then, new experiments have shown that the (√3 x √3)R30° [9,14,15] and c(2x2) structures[16] are generally formed by hydroxyl coadsorption. Adsorption of intact water is much more complex than was anticipated, forming structures that are sensitive to both the chemical nature of the surface and its symmetry. In fact, the 'icelike' bilayer envisaged in Figure 2a has not been observed on any metal surface. Progress in understanding water-metal interfaces has relied on a close interaction between computer simulations, usually density functional theory (DFT), and experiments that deploy the full range of surface structural probes. These new experiments reveal considerable diversity in the structural behavior of water at metal surfaces and new insight into the wetting behavior.

2.2 Low temperature, metastable clusters

When deposited at 4 K water adsorbs as a monomer, adopting a flat geometry, close to the atop metal site[17] so as to optimize the interaction of the $1b_1$ lone pair on O with the metal.[18] STM and vibrational spectroscopy reveal aggregation and clustering at T≥20 K, forming hydrogen bonded networks with long range order above ca. 135 K, depending on the surface. Water sublimes between 160 K (bulk ice) and ca. 180 K in UHV, although water/hydroxyl structures may be stable to 220 K or above, so investigating

metal-water interfaces at higher temperatures requires a static vapor pressure of water, as discussed in sections 3 and 4.

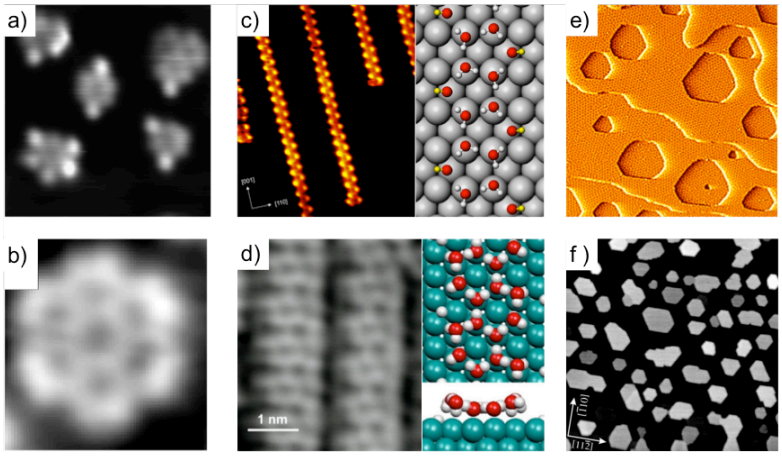

Figure 3. Different types of water structure formed at metal surfaces. 1D clusters on a) Ru(0001) at 130 K and b) Pd(111) at 100 K; 2D chains on c) Cu(110) at 150 K and d) Ru(0001) at 145 K; 2D layer on e) Pt(111) at 140 K; 3D film growth on f) Pt(111) at 140 K. Figures adapted from a) ref [19], b) ref [20], c) ref [10], d) ref [21], e) ref [22]and f) ref [23].

Figure 3 shows STM images of water on several metal surfaces, illustrating the range of adsorption behavior observed. Depending on the metal, and surface temperature, water may form small clusters (0D structures), extended (1D) chains or (2D) networks of hydrogen bonded water molecules. STM experiments are able to manipulate water, assembling clusters of known size and examining their structures by comparison to DFT calculations. On the rectangular Cu(110) surface Kumagai *et al.* [24,25] have found chains of water trimer to hexamer, aligned along the Cu close packed rows. The trimer energetically prefers the "ferroelectric" chain form to a cyclic structure, in spite of the reduced number of hydrogen bonds, highlighting the crucial role of the water-substrate interaction in stabilizing adsorbed water molecules. On the other hand, the cyclic cluster becomes more favorable for the tetramer, as the angle of the hydrogen bonds increases.[24] The close packed metal faces, with their threefold symmetry, give rise to different clusters. STM images of the water dimer on Pt(111) show a star shaped image that is associated with rotation of the asymmetric dimer.[26] One water is bonded flat to the metal while the other water acts as an acceptor, sitting further from the metal and able to hop between adjacent atop sites

around the lower water.[27] Water hexamers are found on the inert, close packed Ag and Cu surfaces.[28] Calculations find that these hexamers are buckled, with three of the water molecules bonded atop the metal and the other three held by hydrogen bonds in a second layer, giving an asymmetric structure with three long and three short hydrogen bonds. The buckling of the hexamer cannot be imaged directly, but further water molecules attach preferentially to the lower water molecules (which are better H donors) to form clusters up to the nonamer.

On more chemically reactive metal surfaces, such as Pd and Ru (which, unlike Ag and Cu, form a wetting layer), the hexamer is bound flat, optimizing the metal water interaction at the expense of forcing the H-bonding angle to 120°.[29] The close match between the metal lattice parameter and the O-O hydrogen bond length allows all 6 water molecules to bind atop the metal, compensating the distortion of the H-bonding network. Addition of a second ring creates one site where the water must adopt a double acceptor geometry; this configuration requires one water to rotate out of plane, sacrificing bonding to the metal surface in order to form two hydrogen bonds. Small clusters containing multiple rings with double acceptor sites have been observed on Pd(111) below 100 K, Figure 3, along with metastable 1D chains of water hexamers.[20] The chains are a kinetic structure, consisting of flat water hexamers, linked into extended chains by a minimum number of water molecules with the double acceptor configuration, a 2D phase forms after extended annealing.

2.3 One dimensional water structures

Whereas the small clusters and chains discussed above are stable only at low temperatures, and coalesce into extended 2D structures when annealed, 1D structures form in preference to 2D networks on Cu(110)[10] and Ru(001)[21]. On Cu(110), water forms extended chains running perpendicular to the close packed rows, restructuring to form a 2D phase only as the surface saturates with water. The short metal spacing on Cu (2.55 Å) hinders formation of hexamer rings, which would have to be compressed laterally by *ca.* 1 Å in order for water to sit in the favored atop site. Instead, water forms a chain of face sharing pentamers, with each pentamer consisting of a four water molecules adsorbed flat atop the Cu and the

final water bound in the double accepter configuration, completing the ring, Figure 3c. On Ru(0001), with its larger lattice parameter (2.65 Å), water forms chains of face sharing water hexamers[21], Figure 3d. Just as on Cu(110), these chains consists of water adsorbed flat, atop the Ru, with one double acceptor water per ring. In both cases the chain structures maximize the water-metal bonding while providing a relatively strong hydrogen bonding network. The reduced H-bond coordination in these chains compared to a 2D network illustrates clearly that the number of hydrogen bonds is not the overriding factor in determining the stability of water structures.

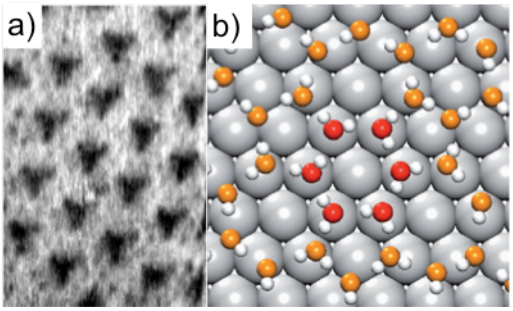

Figure 4. a) STM image of water on Pt(111) and b) structure of the water in the depressions showing formation of a flat hexamer (O atoms in red) linked in to a 5, 7 defect structure (adapted from ref [30]).

2.4 Extended, two dimensional water networks

Having seen that water prefers to form 1D chains instead of a 2D network on some surfaces, it is little surprise that the 2D water phase is more complex than anticipated by the bilayer model, with water forming large, complex unit cells on many close packed surfaces. Images of the saturation √39 and sub-saturation √37 water layers formed on Pt(111)[30] show triangular shaped depressions, separated by hexagonal rings of water that are rotated 30° from the direction expected by simple registry with the metal, Fig 3. Electronic structure calculation indicate the water networks are built from a flat water hexamer, bound tightly to the metal, surrounded by five and seven membered rings that embed the flat hexamer within a hexagonal network of water, where the uncoordinated H atoms point 'H-down' towards the metal surface. This structure allows a strong interaction between the central water hexamer and the metal, and a strong, relatively unstrained hydrogen bonding network. Simulations reproduce the STM

images observed on Pt(111) and are consistent with the flat and H-down water found by X-ray absorption spectroscopy[31] (XAS) and reflection absorption infrared spectroscopy (RAIRS).[32] Structures similar to this unit have been observed in disordered clusters formed on other surfaces[33], giving credence to the idea that this may be a general model for the 2D wetting layer on close packed metal surfaces, at least where the water-metal interaction is relatively weak.

One way to demonstrate the role of the water-metal bonding, and to force water into a simple 2D commensurate bilayer structure, such as in Figure 2, is by alloying the metal to produce a template that is incompatible with other networks. Substituting Sn into Pt(111) creates a Sn template that stabilizes a simple $(\sqrt{3} \times \sqrt{3})R30°$, H-down water bilayer[34], similar to the structure shown in Fig. 2b. This structure is not stable on alloys with a reduced metal spacing[35], implying that the template must match closely the bulk O-O spacing, as predicted by calculations.[36,37]

2.5. Hydroxyl stabilized structures

As indicated earlier, hydroxyl forms easily at metal surfaces, e.g. by partial dissociation, reaction with O, or electron damage, and has a profound influence on the first layer structure. The presence of OH pins the water/hydroxyl structures into registry with the surface, making them easier to image in STM. Pt(111) forms a stoichiometric 2D structure, with a composition of $1OH:1H_2O$, each O atom being surrounded by 3 H atoms to complete a flat hexagonal $(\sqrt{3} \times \sqrt{3})R30°$ hydrogen bonding structure with no uncoordinated H atoms. [9,38,39] Other transition metals show similar commensurate networks, although the OH/H_2O composition appears to vary. [14] On Cu(110) mixed OH/H_2O chains, assembled by manipulation using an STM tip, demonstrate H transfer triggered by vibrational excitation.[40] In the absence of water, OH binds in the short bridge site on Cu, forming $(OH)_2$ dimers with the acceptor pointing away from the surface.[41] Water dissociation is activated, forming a series of structures with different OH/H_2O ratios. The c(2 x 2) structure, which is also seen on other f.c.c.(110) surfaces, consists of a distorted 2D hexagonal network with a composition of *ca.* $2H_2O:1OH$. Instead of forming a complete hydrogen bonding network, the excess water is stabilized by forming a network of flat lying water containing OH Bjerrum defects.[16] This

arrangement maximizes the bonding of water to the metal and the number of strong hydrogen bonds formed by donation to OH. A stoichiometric 1OH:1H_2O phase appears at higher temperature, consisting of water adsorbed flat in a 1D zigzag chain above the close packed Cu rows, with each water donating to an OH bound in the bridge site. This structure allows both species to adopt their optimum adsorption site and geometry, while forming strong hydrogen bonds to water and OH. A common theme of all these studies is that OH is a poor H donor but a good acceptor, so structures involving water and OH will prefer to have water bound flat above the metal, donating H to water or OH at the expense of losing weaker bonds formed by OH donation.[16] The partially dissociated phase formed on Ru(0001) also consists of 1D chains, but the structure is very different[21], consisting of face sharing chains one hexamer wide, decorated by flat, single acceptor water molecules. In this case OH is embedded within the hexagonal chains, enabling the structure to stay flat and maximize the amount of water bonding flat atop Ru. This abrupt change in OH adsorption behavior demonstrates succinctly exactly how sensitively the first layer structure reflects differing water and hydroxyl interaction with the metal substrate.

2.6 Multilayer growth

Based on a better picture of how water behaves in contact with a metal surface, we can ask how multilayer films grow and how the first layer of water is modified to stabilize the thicker ice film. Experiments in this area are less extensive, reflecting the experimental difficulty of characterizing multilayers in detail, but it is clear that the nature of the first layer strongly influences the growth behavior of water multilayers, depending on the ability of the first layer to rearrange and stabilize additional water. Hydrophobic surfaces show a preference to form clusters consisting of two water layers[42], with the water structures showing a complex morphology, not a simple close packed basal plane of ice. The wetting layer formed on the majority of metal surfaces contains a mixture of flat and H-down water[9], with no dangling OH groups available to stabilize second layer adsorption. On surfaces where this layer is tightly bound it will be unfavorable for the water layer to relax during multilayer adsorption. For example, on Ru(0001)[43] and on the mixed OH/H_2O structure formed on Pt(111)[44], the first layer does not wet, instead

water forms 3D clusters that only cover the surface completely when the film is 100's of layers thick. In contrast the mixed OH/H_2O phase on Cu(110) contains excess H atoms, and this surface adsorbs second layer water freely[16], presumably by relaxation of the first layer to stabilize multilayer water. Because the first layer water on Pt(111) is optimized to bond to the metal, with no free OH groups available to act as H donors, multilayer adsorption is initially unfavorable[45], but further water adsorption will reconstruct the first layer to form islands of incommensurate ice, oriented to the metal close packed rows.[46] STM measurements show formation of flat multilayer ice crystallites with a height that reflects the energy cost of restructuring the first layer water to create the bulk ice-Pt interface.[23] Growth of thicker films is enhanced by the formation of screw dislocations which grow by step flow, avoiding the need for a new water layer to nucleate and leading to cubic rather than hexagonal ice.[47]

2.7 Outlook

As the preceding discussion illustrates, the combination of new detailed experiments and DFT calculations has proved a reliable probe of water-metal interfaces, revealing details about the behavior of water from which more general models can be proposed. However, several questions remain. At present our ability to probe the atomic structure of buried interfaces is limited, while we know little about the large unit cell structures that form on rectangular (110) surfaces, such as Cu(110)[48], or the behavior of water on the square fcc(100) surfaces. DFT, even with relatively simple generalized gradient (GGA) approximation functionals has proved reliable in predicting the relative stability of water structures at metal surfaces and reproducing detailed experiments, offers a way to explore systems that are experimentally intractable. However, the GGA functionals widely used have various well-documented shortcomings when it comes to dealing with bulk liquid water[49]. Van der Waals dispersion forces are particularly relevant when seeking to obtain accurate quantitative determinations of adsorption energies.[50,51,52] Aside from working towards improving the accuracy of DFT exchange-correlation functionals[53], an important step forward in this area would be the development of proper quantitative models for the water-surface interaction for specific metals, benchmarked against DFT calculations and

able to reproduce the stability of real structures, to allow new MD models to provide a realistic simulation of specific water-metal interfaces, rather than just the generic solid-water interface modeled presently. An important step forward would be the development of quantitative structural models of water at metals against which DFT could be further benchmarked and classical empirical potentials trained. We will have more to say about this in the next section but the development of more realistic classical potential models for specific water-metal interfaces, rather than the relatively simple generic models currently used, is highly desirable to allow simulations to investigate the variety of behavior exhibited by water at different interfaces.

3. BULK WATER/METAL INTERFACES

After the discussion of low coverage and monolayer water adsorption at low temperatures and under ultra high vacuum conditions we now turn our attention to bulk aqueous solution/metal interfaces, which are of paramount importance to a broad range of scientific and technological areas, including electrochemistry, heterogeneous catalysis and energy storage.[54,55,56,57,58,59] Consequently these interfaces have been investigated for more than 100 years using both experimental and theoretical approaches. While a thorough discussion of the current literature is outside of the scope of this work, Refs. 9, 60, 61, and 62 offer relevant recent reviews.

At ambient conditions, when metal interfaces are in contact with liquid water, the molecular structure of the interface is no longer directly accessible like it is at monolayer coverages and ultrahigh vacuum conditions. Thus, indirect measurements and theory are needed. A number of recent experimental methods have recently provided important insight into water-metal interfaces. For instance, temperature programed desorption of ice-metal interfaces has uncovered a weakly interacting first monolayer of water suggestive of a mostly in-plane hydrogen bonding geometry.[63] Similar weak interactions have been inferred from altered wetting behavior either with un-dissociated water molecules[31] or in mixed water-hydroxyl overlayers.[9] The importance of surface hydroxyl groups for the wettability has been demonstrated for a metal under ambient conditions of relative humidity and temperature: While Cu(110) is covered by a mixed hydroxyl/water layer at a RH of 5%, Cu(111) does not show the presence of molecular water at the same RH, due to the higher dissociation barrier of water on the less reactive (111) surface.[64,65] Electrochemical kinetic measurements with simple kinetic modeling have unveiled the potential for unexpectedly long timescale relaxation times,[66] which is also consistent .with recent probes of electronic relaxation.[67] Recently, x-ray absorption experiences have been preformed at water-gold interfaces under bias, and has unveiled an altered interfacial water structure.[68] Together with first principles modeling, it was determined that applied voltage can shift the number of molecules that are bound to the interface, losing hydrogen bonds to the liquid.

Modeling extended water-metal interfaces at a molecular level is difficult for a number of reasons generic to other aqueous interfaces, as well as many specific problems arising from the structure and dynamics of water at the interface as a result of the subtle balance of water-water and water-substrate interactions. This balance is manifested already at monolayer coverages on simple planar metal surfaces, where STM experiments have exposed a rich variety of two-dimensional hydrogen bonding structures, as discussed in the previous section. At ambient temperatures, where entropic effects mix many of these nearly degenerate configurations, this balance is also evident and can result in a wide range of wetting behaviors from hydrophobic to hydrophilic.[62,69,70] While the intermolecular interactions between water molecules are notoriously difficult to capture, for water-metal interactions a coherent picture of the forces acting on a single molecule on a closed-packed planar surface has emerged over the last 10 years[18,71,72,73,74], but collective effects that arise from multi-body interactions and the influence of step edges (e.g., on higher indexed surfaces) and other defects are largely unknown and unexplored.

Apart from the specifics of the intermolecular interactions, the statistical nature of the liquid state in contact with the metal necessitates an adequate treatment of fluctuations. This means that an ensemble must be sampled, requiring a way of generating many independent configurations which populate an appropriate Boltzmann distribution. Independent configurations are typically generated using molecular dynamics simulations, which can be hampered by long correlation times common for liquids in heterogeneous environments.[75] For most systems of interest the appropriate ensemble fixes the temperature, volume, particle number, and importantly, the applied electric potential within the metal. In practice, molecular dynamics simulations of water near metal interfaces have come in two varieties, either *ab initio* from electronic structure theory or with empirical force fields. In the former, forces are computed "on the fly", typically with DFT.[76] While this approach affords minimal assumptions as to the form of interactions among water molecules, and between water, the metal surface and solutes, the relatively high computational expense limits the system size, although calculations involving thousands of molecules are possible.[77] These two types of simulations are illustrated in Figure 5.

The aim of *ab initio* calculations has, however, primarily been to model chemical bonds and reactions

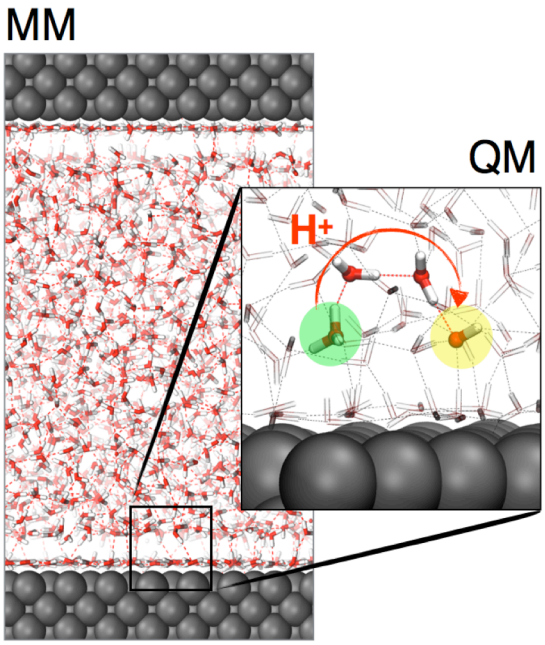

Figure 5. Characteristic snapshots taken from molecular dynamics simulations of the water-platinum interface. These two molecular renderings illustrate roughly the current state of the art with regard to simulation sizes approachable with empirical molecular mechanics (MM) and *ab initio* forces (QM). Empirical models are capable of simulating 10^4-10^5 molecules over hundreds of ns, while *ab initio* models are capable of following 10^2-10^3 molecules over 10-100 ps. However, only the latter is able to capture chemical bonding rearrangements necessary for a complete description of electrochemically relevant phenomena.

rather than dynamic properties of interfacial water. *Ab initio* models have previously suffered difficulties in the numerical description of water due to the strong non-bonding interactions. The numerical description of the interaction of water molecules on a metal surface has traditionally met more success.[76,78] Differences in adsorption energies on metal surfaces appear to be generally well described by DFT with standard GGA functionals such as PBE[79] and RPBE[80], which are computationally relatively inexpensive. For example, ground state structures predicted at this level of theory for monolayer and sub-monolayer coverages are typically in good agreement with those observed in low-temperature STM experiments.[10,81,82] However, various functionals which account for van der Waals dispersion forces have recently been developed and applied to water/solid interfaces.[83,84,85,86] These functionals are expected to

provide a more balanced description of water-water versus water-surface interactions and have been shown to improve the wetting properties of water monolayers on metals.[87] Most importantly, *ab initio* calculations of water/metal interfaces are able to describe instances of dissociative adsorption and mixed water-hydroxide or water-hydride interfaces. Many recent studies have exploited that benefit as well as exploring the structure and dynamics of aqueous water-/metal interfaces (although we caution that with AIMD simulations relatively small system sizes and/or short dynamical trajectories are a necessary evil).[76,88,89,90,91,92,93,94]

The modeling of electrochemical reactions at the metal-water interface requires to allow for the exchange of species like protons or counter ions (rather than working with a constant number of particles), which is not straightforward in molecular dynamics simulations.[95] In addition, the modeling of electrochemical interfaces poses additional challenges related to the applied potential[68] and the electrochemical environment.[96] In recent years, a number of small advances have been made towards *ab initio* models that include these features.[88,97,98,99]The general challenge is that the simulation of open quantum systems is exponentially complex. Grand canonical ensembles with continuously varying numbers of electrons have been consistently formulated within a DFT framework[100,101,102,103], however, these methods have not yet garnered widespread use largely due to their computational complexity. Other more practical methods have been developed specifically aimed at static electrochemistry. These methods use an *a posteriori* mapping from fixed charged calculations to a Grand Canonical ensemble. Here the electron work function is taken as a measure of the electrode potential or electron free energy.[92,104,105,106]

These systems are still not in equilibrium with the ionic chemical potentials, since the number of ions is kept constant. Nevertheless, it is possible to measure pH and potentials in a simulation using the work function as potential scale and a variable number of protons in the simulation cell. By doing so it has been observed that changing the pH at a fixed driving force can cause water to reorient at the interface.[89] By combining small monolayer calculations with continuum dielectric theory, in the form of Poisson-Boltzmann theory, Jinnouchi and Anderson[104] were able to accurately compute the potential of zero charge of the water-platinum electrode. Electrochemical reactions including charge transfer across the

water-metal interface and its dependence on the interfacial water structure can now be calculated with *ab initio* models. Such studies have started to appear within the last decade.[88,99]

While most *ab initio* calculations of liquid water near extended metal interfaces are fairly recent, there is a long history of studies using classical molecular dynamics simulations based on empirical force fields. These studies typically use static electronic structure calculations to parameterize intermolecular potentials and are able to handle systems of 10^4 to 10^5 molecules and trajectories of 10-100 ns. While many intermolecular potentials for water exist, only a few different potentials for the water-metal interface are routinely used. 92,[107] These potentials usually recover the single molecule binding energies and diffusion barriers with good accuracy.[92,108] However, they are mostly unable to reproduce the complex ground state structures of single monolayers, unlike *ab initio* models which accurately describe both water-water and water-metal interactions.[69,109] Moreover, most classical models are also not flexible enough to easily incorporate bond breaking and charge transfer, though there has been success in adapting Empirical Valence Bond models to describe the dynamics of excess protons near the water-metal interface through multi-state approaches.[110,111,112,113,114] The utility of a force-field based approach is that collective effects from the correlated dynamics of many molecules can be sampled and subsequently thermodynamic properties can be computed with reasonable assurance as to their statistical convergence. This has enabled studies of water orientational dynamics[110,115,116], ionic adsorption[117,118,119] and solvation[69,120,121] within the interface. These studies have been largely limited to defect-free low index fcc surfaces due to the complexity of the interactions at defect sites. Further, they have also been largely constrained to instances where dissociative adsorption does not occur, at least at low temperatures.

The relevance of these studies for a better understanding of electrochemical reactions has been increased by methods that sample a constant electric potential ensemble and combine that with rare event methods.[122] The most widespread and versatile method for doing this was developed by Seipmann and Sprik[109] for studying interactions of water adlayers with an STM tip and adapted to electrochemical cell calculations by Madden and coworkers.[123] In this treatment the charge distribution on each electrode changes dynamically, subject to a constraint of a fixed electrostatic potential. By monitoring the charge

fluctuations on a given electrode, the Johnson-Nyquist relation allows for the facile calculation of the capacitance of the cell[124,125]. These calculations are capable of recovering known capacitances and potential drops across the interface and have also provided a useful means for testing fundamental assumptions about the mechanisms, driving forces and timescales of electron transfer and liquid reorganization.[126,127] Specifically, by computing vertical energy gaps for standard redox couples at various distances from the electrode, Willard *et al*. have shown that energy gaps are Gaussian as expected from Marcus theory, and that the reorganization energy includes terms from the solvent dielectric as well as unscreened image charges on the electrode.[128] Limmer *et al*. have found that constraints on strongly adsorbed interfacial water can result in a hierarchy of timescales of solvent motion, ranging from the ps relaxation times of bulk density fluctuations to 10-100 ns for dipolar fluctuations of water within the adlayer.[69] These fluctuations are important to the chemistry at metal/solution interfaces, as slow polarization fluctuations within the solvent couple to charge reorganization; simulation approaches that are not able to reach these relaxation times lead to results that are difficult to interpret.

There are a number of efforts to combine the accuracy provided by *ab initio* methods in describing water-metal interfaces, including bond formation and breaking as well as charge transfer, with the computational tractability afforded by classical molecular dynamics, in particular their ability to describe long range correlations and slow dynamical processes. Recently Golze *et al*. have implemented a method for including polarization effects in hybrid quantum mechanics/molecular mechanics simulations of adsorbate-metal systems.[110] This method provides a density functional theory treatment of liquid water, combined with an empirical force model for the water-platinum interaction that includes polarization fluctuations on the metal with the correct constant potential ensemble. This method mitigates the complexity associated with the electronic structure of the metal, while allowing for bond-breaking within the liquid. Voth and co-workers have employed force matching to parameterize reactive models of water that include excess protons and hydroxide, which could be used together with generalized water-metal potentials to study dissociative adsorption.[117,129] An attractive avenue for further pursuit is to generate potentials using neural networks[130] or other machine learning approaches [131] or many-body expansions[132]

which offer a higher degree of flexibility over standard force field approaches and could be used to parameterize molecular forces fields for a description of water-metal interactions with higher level electronic structure theory than used previously. These mixed quantum classical calculations may offer the potential to advance the modeling of water-metal interfaces in the short term, while full *ab initio* descriptions for now are confined to limited system size.

4. WATER/OXIDE INTERFACES

Water/oxide interfaces impact many natural processes, for example the hydrodynamic properties of Earth's subsurface or cloud nucleation in the atmosphere.[133,134,135] Fuel cells, solar-energy production and catalysis are a few examples of technological applications where the oxide/water interface plays a crucial role.

In particular thin water films are important in many environmental reactions and technical applications since at ambient relative humidities thin water or solution layers will cover most surfaces (see Fig. 1c), and a large majority of solid surfaces in the environment and technical applications are oxides, since the vast majority of metals and semiconductors are terminated by a native oxide layer under ambient conditions. Section 2 showed that our understanding of the structure and properties of thin water layers on metals at low temperatures has advanced considerably over the last decades. Due to their ubiquity and importance for environmental and technological processes it is of great importance to expand this atomic level understanding to aqueous films under ambient conditions of temperature and

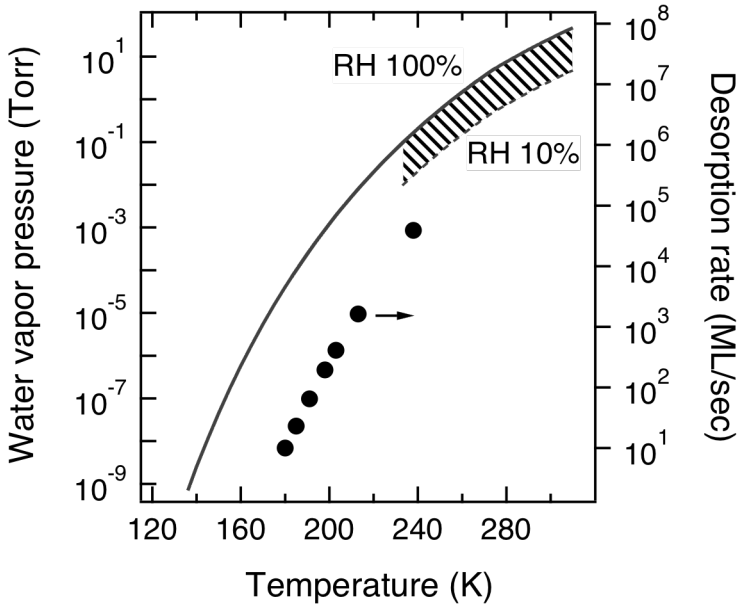

Figure 6. Equilibrium water vapor pressure as a function of temperature (solid line). The water vapor pressure for a relative humidity of 10 % is also shown for ambient temperatures. Measured desorption rates from ice, taken from Ref. , are shown as solid circles. These data show the two obstacles that experiments under ambient relative humidity face: high background pressures of water vapor, and rapid condensation/evaporation rates for bulk liquid and ice samples upon deviation from the equilibrium relative humidity.

water vapor pressure. The main experimental challenges in such investigations are the elevated vapor pressure of water and the high adsorption/desorption rates, as shown in Fig. 6. Most experiments on thin water films where performed at temperatures below 200 K (see section 2), where the water vapor pressure is negligible. If one defines ambient temperatures as those above 240 K, then the measurements have to be performed in the milli-Torr to tens of Torr water vapor partial pressure range, lest the films evaporate from the surface. Over the last decades a range of surface sensitive techniques that are able to operate under these non-UHV conditions has been developed, including infrared and non-linear optical spectroscopy[136], scanning probe microscopy[137], and X-ray based core level spectroscopies[138], to name a few. Structural insight into interfacial water on oxide surfaces on the molecular scale is gained through the use of surface sensitive X-ray diffraction methods. [139,142] It is not only considerably more challenging to investigate water adsorption on oxide surfaces under ambient conditions experimentally, but also computationally. As briefly touched upon in the previous section, DFT studies are hampered by the fact that it is not trivial to include macroscopic variables, such as pH and the electrostatic potential, in the models. However, a number of molecular dynamics simulations with classical or *ab initio* force fields do provide structural information which can be interpreted essentially as valid in an environment with undefined electrochemical variables.

4.1 Open questions

Some of the main open questions in these studies are molecular vs. dissociative water adsorption, the onset relative humidity for water adsorption and the possible formation of hydroxyl layers, the influence of the presence of contamination layers on water adsorption, and the influence of the presence of hydroxide/molecular water layers on the reactivity of the substrate towards gas phase molecules. Another important question is the influence of the substrate on the water layer structure and properties, *i.e.*, at which layer thickness do the properties of the thin film converge with those of bulk water (see Fig. 7). Conversely, one can consider the properties of the ultrathin liquid films from the point of view of those of a bulk solution/solid and bulk solution/gas interface (discussed in section 6): At which bulk solution

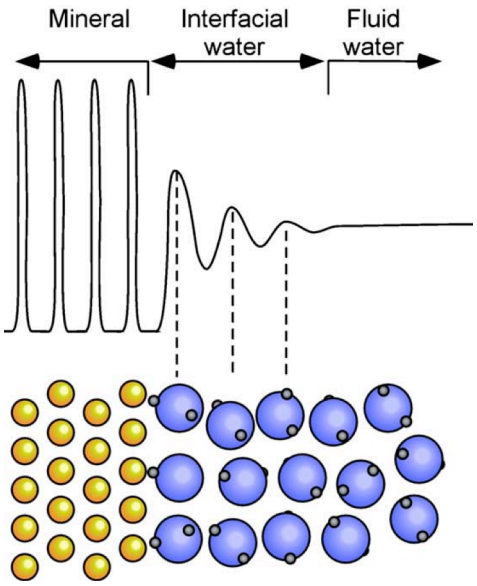

Figure 7. Microscopic perturbations to the average water density as a function of distance to an interface. These perturbations usually decay within 10Å of the surface. Reprinted from Ref. 139.

thickness do the chemical and physical properties of the solid/liquid interface influence those of the liquid/vapor interface, and vice versa? Given that the thickness of many solution layers on oxide surfaces under ambient relative humidity is of the order of a few nanometers or less, this is an important question for the understanding of the heterogeneous chemistry of surfaces under realistic environmental conditions. We have taken only small steps in our basic understanding of these questions so far.

Electrochemical experiments and theoretical continuum electrostatic models have been applied for many decades to characterize interfacial water on oxide/solution interfaces, in particular the electric double layer. One of the most important macroscopic quantities, the dielectric constant, is reported to be an order of magnitude lower on the interface compared to bulk water: On mica, for example, it is ~4 at the interface compared to ~78 in bulk water.[140] This can be rationalized by interactions between water molecules with the electric field at the oxide/solution interface. The dielectric constant is thus expected to vary dramatically for interfaces with a strong reordering interaction compared to those with weak perturbations to the bulk properties. Yet, the dielectric constant is a macroscopic property, and like other continuum variables, it does not provide a satisfactory microscopic description. Despite their long history, electrochemical methods are an indirect way to probe the solution/solid interface, since they only directly

detect charge transfer to and from the electrodes, and no direct information on the interfacial water structure.

In this section we will limit the discussion to some of the most stable oxide surfaces that have been widely studied both experimentally and theoretically: Mica, SiO_2, Fe_2O_3, Al_2O_3, MgO and TiO_2. For broader recent reviews on the subject see, e.g., Refs. 141 and 142.

4.2 Mica

We first consider the formation of non-dissociative water adsorption and the influence of the substrate on the structure of the first monolayer of water. One of the most widely studied surface is muscovite mica, which is a layered alumino-silicate. Extended, flat (0001) basal plane surfaces can be prepared by cleaving using adhesive tape, owing to the weak bonding between adjacent $(Al,Si)O_2$ layers. Early first principle molecular dynamics simulations (involving a small simulation cell and a very short dynamical trajectory) showed a strong templating effect of the mica(0001) surface on the first water layer (see Fig. 8), which forms a two-dimensional hydrogen bonded network with a preferential orientation of hydrogen-donor bonds of the adsorbed water with the oxygens in the mica surface.[143] This leads to a structure of the first water monolayer without any dangling H-bonds and with a net dipole moment with the positive

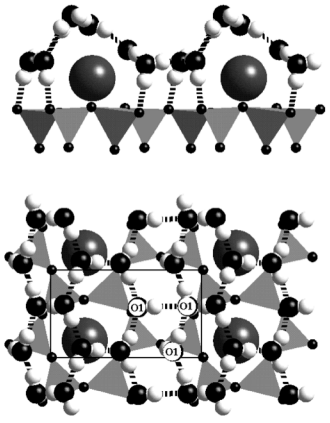

Figure 8. Side and top view of the optimized structure of a water monolayer on muscovite mica obtained from ab initio molecular dynamics simulations. Dashed lines are hydrogen bonds, while black, white, and gray spheres depict oxygen, hydrogen, and potassium atoms, respectively. An ordered 2D ice-like structure forms on the mica surface. [Reprinted with permission from Ref. 143. Copyright 1997 by the American Physical Society.

end pointing towards the surface. This model has been confirmed using SFG[144] and Kelvin probe microscopy[145], which showed that there are no detectable dangling OH bonds at relative humidities below ~80% (i.e., below the monolayer coverage)[144] and that the surface potential of mica decreases upon adsorption of water[145], in agreement with the orientation of the water dipoles with the positive end towards the substrate. The SFG measurements also showed that at higher relative humidities, where multilayer water is present, dangling OH bonds are observed, hinting at a certain degree of disorder in the second layer, where some of the order in the first layer is lost, at least at measurement at room temperature.

Strong templating, like the one described above for mica, has also been observed for water monolayers on non-oxide surfaces, e.g. $BaF_2(111)$ using a combination of near edge X-ray absorption fine structure spectroscopy and MD simulations.[146] $BaF_2(111)$ has been widely studied in view of the close match of its lattice constant to that of the ice I*h* (0001) basal plane.[147] The recent combined polarization-dependent NEXAFS and MD investigations by Kaya et al. reveal that the first monolayer of water on $BaF_2(111)$ shows an unusually high density (1.23 g/cm^3).[146] This high density is due to a very narrow distribution of the water molecules in the first layer in the direction perpendicular to the $BaF_2(111)$ surface, as well as a collapse of the 2nd coordination shell within this layer, with a O-O distance of ~3.3 Å compared to 4.4 Å for bulk water. This small 2nd coordination shell radius is comparable to that for very high density water (VHDL), only that in the case of the water monolayer on $BaF_2(111)$ the surface itself provides the driving force for the compression of the layer.

We now return to the discussion of the water/mica interface and consider the templating effect of the mica surface on adjacent water in the presence of bulk water, which was demonstrated in a high-resolution X-ray reflectivity study.[148] Oscillations in the water oxygen density in the direction normal to the surface provided evidence of interfacial water ordering, in quantitative agreement with a later Monte Carlo study.[149] The density distribution of water oxygen atoms at the interface shows more than four distinguishable peaks, where the two water layers closest to the mica interface have an oxygen density that is about twice that of bulk water. At the same time, the water density does not drop well below the

bulk density at any point, leading to an overall increased water density at the mica interface as discussed for BaF_2(111) above. The density oscillations are observed at a distance of within about 1 nm from the interface. Even though there is strong ordering of water and an increase in the density of water at the mica/water interface, molecular dynamics calculations of the shear dynamics of water layers with thicknesses <2.5 nm confined between two mica surfaces show a high fluidity of the interfacial layers.[150] This surprising finding was explained by the persistent mobility of water in the hydration layer through fast rotational and translational dynamics of water molecules.[150]

4.3 Silica

Micas are a two dimensional subspecies of the much more widely found and important silica minerals (SiO_2) which are the main component of the Earth's crust. Freshly cleaved silica exhibits coordinatively unsaturated Si-O bonds, which will react rapidly with atmospheric moisture, leading to the formation of surface (Si-OH) groups. The interfacial layer at the silica/water interface was experimentally explored by, e.g., SFG which revealed that the orientation of interfacial water molecules were strongly affected by electrostatic interactions and hydrogen bonding to the oxygen in the quartz surface.[136,151] Theoretical studies of the silica/water interface focused, e.g., on the acid-base chemistry of silica surfaces using *ab initio* molecular dynamics on multiple representative crystalline silica surfaces.[152] These studies revealed that silanol groups are only present on strained or defective surfaces, with a pKa of ~4.5. Classical MD simulations of the structural and dynamical properties of water at hydroxylated silica surfaces showed a slower dynamics of interfacial water compared to that of the bulk.[153]

4.4 MgO

We now turn our attention to the dissociative adsorption of water on oxide surfaces at ambient relative humidities, and the effect of surface hydroxyl groups on the hydroscopic properties of the oxide. Many of these studies were performed using ambient pressure X-ray photoelectron spectroscopy (APXPS)[154,155 156], which can operate at pressures in the Torr range, and is an excellent method to

determine the onset relative humidity (RH) for hydroxylation and water adsorption, since it can distinguish between oxide, hydroxide and molecular water species *via* their different "chemical shifts" in O 1s photoelectron spectra. Over the past decade APXPS was been used to study water adsorption on the single-crystalline oxide surfaces of $TiO_2(110)$[157], α-$Fe_2O_3(0001)$[158], $Fe_3O_4(001)$[159], thin film $MgO(100)/Ag(100)$[160,161], and on thermally-grown or native oxides of $SiO_2/Si(111)$[162], Al_2O_3/Al[163], $Al_2O_3/NiAl$[164]and $Cu_2O/Cu(111)$[165]. Figure 9 shows results of APXPS measurements of the reaction of water vapor with MgO(100), arguably one of the most closely studied surface in terms of water adsorption, both theoretically[166,167] and experimentally. The APXPS and IR data (adapted from Refs. 161 and 168, respectively) show that hydroxylation and water adsorption starts at RH<0.1 %. While the growth of the hydroxide layer terminates at ~ 1 ML at a RH of ~0.1 %, the thickness of the water layer increases with increasing RH, reaching 1-2 MLs at ~20 % RH. The concomitant stabilization of significant amounts of molecular water on the MgO(001) surface with the onset of hydroxylation

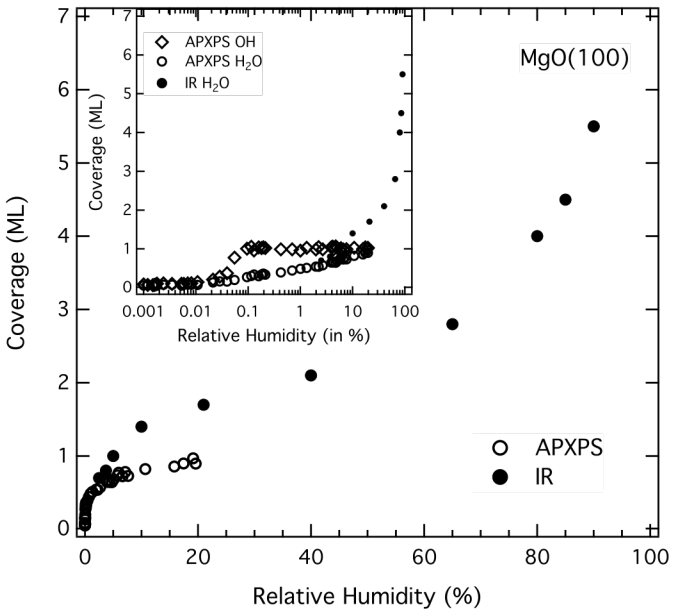

Figure 9. Water film thickness as a function of relative humidity on MgO(0001) as measured by APXPS (open circles) and IR spectroscopy (filled circles). The inset shows a close-up of the low RH region, plotted vs. the log of RH, with the thickness of the hydroxylated layer on MgO(0001) shown as open diamonds. The APXPS data show an onset for hydroxylation and water adsorption on α-$Fe_2O_3(0001)$ already below 0.1 % RH. Both IR and APXPS show the presence of a ~1-2 ML thick water layer at RH above 20 % RH. Data adapted and reproduced with permission from Ref. [161] (APXPS) and Ref. [168] (IR).

underlines the importance of OH-H_2O bonding (which are stronger than H_2O-H_2O bonds) during the initial stages of water adsorption.

4.5 TiO_2

Another important oxide/water interface where the formation and role of hydroxyls has widely been discussed is the TiO_2/water interface.[169] TiO_2 occurs in three crystal structures: rutile, anatase and brookite. Of these, rutile has been studied the most, especially its most stable face, i.e. (110). There is strong experimental evidence that water dissociation occurs at defect sites (see e.g. ref. [170]) The results of theoretical studies of water on the defect free surface, in particular the question of intact versus dissociative adsorption has been hotly debated.[171,172,173,174,175,176,177,178] This has been a controversial issue mainly because the energetic difference between the intact and dissociated water molecule states is very small (<0.1eV). As a consequence the relative energy of the states depends sensitively on the details of the computational set-up used; most notable the thickness of the simulation slab and the exchange-correlation functional. The debate of how water adsorbs is not limited to single water molecule adsorption, but extends to monolayer adsorption as well as thicker water films on rutile(110). Figure 10 illustrates the challenge faced by theory in predicting whether or not water dissociates on the pristine TiO_2(110) surface by revealing the relative energy of intact versus dissociated water as a function of the number of layers in a TiO_2 slab. Strong oscillations can be observed with the prediction of whether molecular or dissociative adsorption is favored exhibiting an odd-even oscillation. Oscillations, essentially quantum size effects, such as this are well known and understood for TiO_2.[179] It is clear from Fig. 10 that the 'amplitude' of the oscillations also depends on the particular exchange-correlation functional used and this goes some way to explaining apparently contradictory results. Nonetheless it is clear from Fig. 10 that with sufficiently thick slabs all functionals considered predict that intact water is thermodynamically more stable than dissociated water on the pristine surface. Liu et al. ran large *ab initio* MD simulations of a thin water film on rutile revealing important information about the structure of the interface: water formed a well-defined contact layer in which water molecules bonded to Ti sites of the

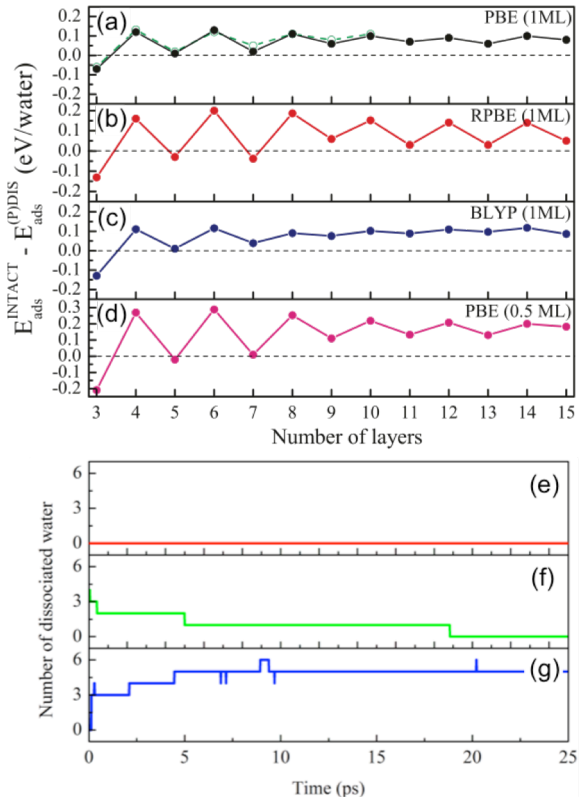

Figure 10. Computed energy differences between intact and partially (1 monolayer, ML) or fully (0.5 ML) dissociated states versus number of TiO2 layers in a slab model of TiO2. A layer of TiO2 is defined as one O-Ti-O trilayer. (a) PBE at 1 ML. (b) RPBE at 1 ML. (c) BLYP at 1 ML. (d) PBE at 0.5 ML. Number of dissociated water molecules at the TiO2 surface as a function of simulation time for three ab initio molecular dynamics simulations at a coverage of 1 ML. (e) An overlayer of intact water molecules on a four-layer TiO2 slab. No dissociation takes place during the simulation. (f) An overlayer on a four-layer slab with four out of the eight water molecules initially dissociated. As the simulation progresses, water molecules recombine until at about 20 ps no dissociated water molecules remain (i.e., all adsorbed OH and H groups recombine). (g) An overlayer of initially intact water molecules on a three-layer slab. Unlike on the four-layer slab, dissociation of water molecules is quickly observed. Results are for the PBE functional at 360 K. The figures illustrate how both at low coverage (top panel) and for a liquid film whether water dissociates or not is extremely sensitive to the slab model used to represent the TiO_2 surface. Top panel taken from Ref. 180 and bottom panel from Ref. 181.

substrate.[180,181] Due to this strong bonding to the surface, water in the first interfacial layer moved considerably more slowly than water molecules in the layers above it. The exchange dynamics between water molecules in the first and second water overlayer agreed well with electron stimulated desorption measurements.[182] An intact non-dissociated water film emerged when Liu et al. used a sufficiently thick (4-layer TiO_2 slab) and indeed on this slab even when water molecules were manually pre-dissociated

water molecules recombined during the course of the *ab initio* MD simulation, as shown in Fig. 10(f).[180] In contrast, and consistent with the simulations at ≤1 ML, if an insufficiently thick 3-layer TiO_2 slab is used to support the liquid water film, water molecules dissociate (Fig. 10(g)). Overall this reveals how incredibly sensitive the structure and dissociation state of water on rutile TiO2(110) is to the precise details of the computational set-up used and certainly there is still scope for improving upon the *ab initio* MD studies of this system that have been performed so far. Nevertheless, an important area where improvements have been made is in the ab initio modeling of the aqueous interface under finite pH. The delicate balance between intact and dissociative water adsorption may be altered by the value of the pH. Cheng et al.[148] have investigated the role of pH using free energy perturbation methods to compute the dissociation constant from *ab initio* MD simulations. However, they found that water dissociation is 0.6 eV less stable than intact adsorption under standard pH conditions, in agreement with the conclusion drawn from Fig.10.

4.6 Thin solution layers on hematite: A case study

Ultrathin water films under ambient conditions can contain dissolved ions and will almost invariably be in contact with carbonaceous material, through reaction with, e.g., CO_2 from the atmosphere, or adsorption of surfactants. For a better understanding of the influence of these contaminants in the adsorbed water layers, it is essential to determine their chemical state and relative location within the adsorbed layer with respect to the solution/solid interface and solution/gas interface. The properties of bulk solid/liquid and liquid/vapor interfaces will be discussed below in this chapter; here we focus on solution layers with thicknesses of a few nm or less, as they will be present at relative humidities below 100%. A recently introduced combination of APXPS with the standing wave (SW) method is a promising strategy to investigate these thin films with depth (SW) and chemical (XPS) resolution.[183] The

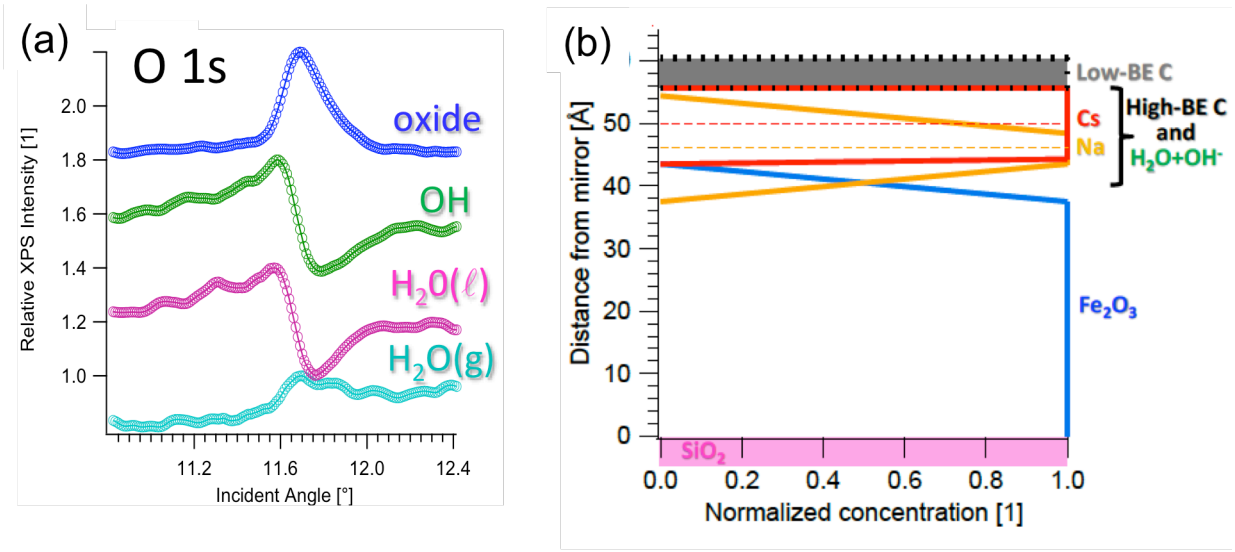

Figure 11. **(a)** O 1s rocking curves from a (Cs,Na)OH thin film deposited on a hematite thin film sample, which in turn was grown on a 3.4 nm period Mo-Si multilayer sample. The relative humidity during the measurement is 8%. The incident photon energy is 910 eV, resulting in a 1st order Bragg angle of ~11.7 deg. The differences in the oxide and OH/H_2O rocking curve peak position and shape indicates that these species are at different positions above the multilayer grating. **(b)** The analysis of the Cs 4d, Na 2p, C 1s , O 1s and Fe 2p rocking curves provides the spatial distribution of the different components as a function of distance above the multilayer, with Na in close proximity to the hematite/solution film interface. A hydrophilic carbon species (carbonate) is evenly distributed throughout the film, while a hydrophobic component is located at the solution/vapor interface. Data adapted and reproduced with permission from Ref. 183.

exciting X-ray wave field is tailored into a standing wave by interference of the incident and reflected X-rays under the first Bragg angle, e.g. off a multilayer grating, where the standing wave has a wavelength of about that of the multilayer periodicity. The standing wave is scanned through the interface of interest (e.g., by varying the incident angle around the Bragg angle in a rocking curve) and thus provides much increased depth-resolution in XPS experiments.[184] The advantage of the standing wave approach is that it provides a built-in ruler, *i.e.*, the period of the standing wave, to determine absolute depth distributions of chemical species throughout the probed volume. Using this method Nemšák et al. have investigated a mixed CsOH/NaOH solution layer on a polycrystalline hematite substrate at a relative humidity of 8 %.[183] The results showed that Na is bound to the hematite surface, while the Cs was excluded from the solid/liquid interface (see Fig. 11). A promising observation in this study is that two different carbon species could be distinguished: one hydrophilic (carbonate or carboxylic acid) that is distributed throughout the solution film and another hydrophobic (aliphatic carbon), which is located in a narrow layer at the solution/vapor interface. The results of this study are an encouraging first step towards the elucidation of the role of ubiquitous hydrocarbon species in the surface and interfacial chemistry of thin water films as well as bulk water/solid interfaces.

4.7 Bulk solution/oxide interfaces

In the following we will discuss bulk solution/oxide interfaces. The experimental study of bulk water/oxide interfaces has mostly been performed by non-linear optical spectroscopy and X-ray diffraction methods, often in combination with theoretical modeling. For the case of hematite a variety of surface terminations have been found, and thus the structure of interfacial water is also expected to be diverse, depending on the termination.[139] Crystal Truncation Rod diffraction and DFT calculations[185] suggest that the hydrated (0001) surface at a $p(H_2O)$ of 10^{-4} Torr or higher at room temperature is hydroxylated, which is in agreement with the previously mentioned APXPS data[158]. Systematic studies of the interfacial water layer in the presence of bulk water and as a function of the surface crystallography were performed by Catalano et al. using X-ray reflectivity on the (012), (110) and (001) facets.[186] These

studies all show a dense hydration layer in contact with hematite, with a gradual transition from a layered structure to bulk properties occurring within the first 1 nm (equivalent to ~3-4 layers) from the surface. This is analogous to the interfacial water layer observed for mica.[148] Force field molecular dynamics simulations provided more details about the nature of the water/hematite interface. They show in particular stable linear hydrogen bonds from water in the liquid phase donated to triply coordinated surface oxygen on the hematite (012) and (110) facets.[187] The (001) facet shows a weaker reordering of the water layer. The interfacial water has been less studied on for iron oxyhydroxides, in particular goethite (FeOOH), which is one of the most important minerals in the environment[188], and it is highly likely that hematite is covered by an oxyhydroxides layers under humid conditions or when in contact with bulk water.

The most common aluminum oxide is α-alumina (Al_2O_3). It has the same crystal structure as hematite and is thus a good test case for distinguishing between the role of crystal structure and surface chemistry in view of the interaction of the surface with water. Alumina is hydroxylated at much higher relative humidities than iron oxides, and vapor/oxide studies show a much weaker layering of water on α–alumina compared to iron oxide, with a thinner interface region.[139,185] Ab initio molecular dynamics simulations of water on α–Al_2O_3(0001) and water on AlOOH(101) provide some new insights into the interaction between surface hydroxyls and the interfacial water[189,190],with surface hydroxyls donating and receiving bonds from water molecules, causing a weak lateral and surface normal water reordering. Force field studies parameterized for α–Al_2O_3(0001)[191] predict better wetting on a hydroxylated surface compared to an aluminum-terminated surface, in agreement with ab initio studies and Monte Carlo simulations with force field potentials.[192]

In summary, common features of interfacial water on oxide surfaces include the width of the interfacial (structured) region to be ~10 to 30 Å, with a slower dynamic for the first water layer directly in contact with the oxide surface. It is also well established from experiments and simulations, that the molecular orientation of interfacial water is governed by the pH, by the surface charge and the

electrostatic environment and by the presence of ions. The explicit inclusion of these factors in numerical simulations is still a challenge. In addition, most simulations are using classical force fields, which are parameterized to reproduce experimental results on a particular material and particular facet. *Ab initio* approaches are still computationally expensive if they are to reproduce long range effects in water, although they have gained ground rapidly over the last five years. Certainly our understanding about lateral ordering is still limited, and also a great challenge in experiments. For the limiting case of ultrathin water layers on oxide surface a picture emerges in which hydroxylation and molecular water adsorption occurs on mot oxide surfaces at relative humidities far below those encountered in the environment (<1%), with consequences for, e.g., weathering of rocks and cloud nucleation processes.

5. WATER AT HYDROPHOBIC SURFACES

After the discussion of the interaction of water with the overwhelmingly hydrophilic oxide surfaces, we now turn our attention to hydrophobic interfaces. The molecular structure of water next to extended hydrophobic surfaces is crucial for understanding hydrophobic interactions ubiquitous in technology applications and biological systems, from the phase separation in oil and water mixtures, to the vital mechanisms that control protein folding. In contrast to water molecules surrounding small hydrophobic solutes, where relative to the bulk no breaking of hydrogen bonds is required, in extended hydrophobic surfaces, interfacial water molecules have no other option but to sacrifice, on average, less than one hydrogen bond per molecule.[193,194] The corresponding non-hydrogen bonded OH group is then expected to point towards the hydrophobic surface, much like at the liquid/vapor interface (see next section).

Experimental evidence for that interfacial water molecules have a broken hydrogen bond or "free OH" has been obtained using vibrational sum frequency spectroscopy.[195] The existence of water

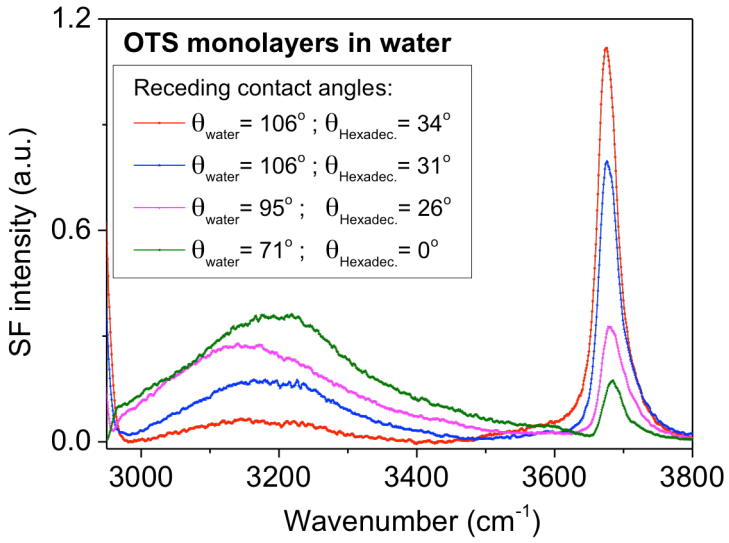

Figure 12. Sum Frequency spectra in the OH stretching region of four hydrophobized silica/water interfaces with varying degrees of order. Silica surfaces were hydrophobized by self-assembly of octadecyltrichlorosilane monolayers. Receding contact angles in water (θ_{water}) and specially hexadecane ($\theta_{Hexadec}$) appear to correlate with the order and/or defects in the monolayer, with the most ordered layer displaying the highest values. The average error in contact angles is ±2-3°. Spectra were collected under the SSP polarization combination and the solid lines are guides to the eye joining consecutive data points. Figure adapted from reference 200.

molecules with a single dangling OH bond next to a hydrophobic surface is unambiguously observed by the presence of a relatively sharp band in the sum frequency spectrum centered at ~3680 cm^{-1} (see for example Figure 12). The fact that only a single band is observed rules out the presence of water molecules with two dangling OHs at the interface. First observed by Shen and co-workers more than 20 years ago[196], this feature has been reproduced numerous times by others[197,198,199,200], although the exact peak position varies depending on the nature of chemical groups exposed by the hydrophobic surface.[197] Besides the sharp dangling OH peak, a broader band is usually observed at lower frequencies in the sum frequency spectrum and is assigned to interfacial water molecules forming hydrogen bonds of varying strength and coordination. This is particularly true for the most frequently used model system for probing the hydrophobic/water interface, which consist of silica substrates hydrophobically modified by self-assembled alkyl silane monolayers (see for example Figure 12 for the lowest receding contact angles). The presence of this broad band at a relatively low wavenumbers (~3200 cm^{-1}) assigned to molecules forming strong hydrogen bonds, was originally interpreted as the ability of the hydrophobic medium to induce order beyond the first monolayer of interfacial water molecules.[196] However, this interpretation has been put in doubt by a number of recent studies. Firstly, sum frequency spectroscopy measurements at varying pHs at the alkyl silane hydrophobic interface have suggested that the effects observed in the bonded OH region are not due to the interactions of water with the hydrophobic monolayer, but are instead a consequence of the underlying fused silica substrate.[199] Secondly, the addition of high concentrations of non-specific adsorbing ions results in an almost total cancellation of the broad OH stretching band, consistent with the screening of the field originating from the charged silica surface.[197] This latter study also concluded that water access to the solid substrate is granted through defects in the self assembled monolayer and not through penetration of the monolayer alkyl chains.[197] Finally, measurements on hydrophobic monolayers of various degrees of order have shown that the broad OH feature in pure water practically vanishes for defect-free alkyl silane monolayers, while at the same time the intensity of the dangling OH increases (see Figure 12).[200] Since the remaining features in the spectrum are primarily linked to water molecules having a dangling OH, these results provide conclusive evidence

that bulk isotropic properties are already present at sub-nanometer distances from the surface of well-ordered hydrophobic monolayers: the induced ordering of water molecules is essentially limited to the first monolayer[200] (notice that sum frequency spectroscopy remains insensitive to water molecules having both their OH bonds aligned parallel to the surface plane). In the same studies an apparent correlation was found between the interfacial molecular properties and macroscopic receding contact angle measurements, and in particular those measured in hexadecane (see Figure 12).[200] It should be noted that no such correlation was found with the static and advancing contact angles in water. Contact angles are commonly used as a macroscopic measure to quantify hydrophobicity.[193]

The fact that the surface induced order is essentially limited to the first water layer has important implications. One such case is regarding the origin of the attractive hydrophobic interaction between two hydrophobic surfaces. This interaction that is inherently due to the hydrophobicity of the surfaces ("true hydrophobic force") becomes detectable at distances in the order of 10-20 nm when using force measuring techniques.[193,201,202] Atomic force microscopy measurements between surfaces of various degrees of hydrophobicity (as estimated by their static contact angles) prepared by either, silane or thiol chemistry, show that the strength and range of the attraction increases with the contact angle.[203,204] One mechanism that has been put forward to explain the origin of this attractive force is associated to changes in the ordering of water molecules between the two approaching surfaces.[193,205] The vibrational spectroscopy results presented above, alas, for a single interface, suggest on the contrary that the order of water molecules at a distance of just a few Å from the most hydrophobic surface (as judged by its receding contact angle), is not different from that in the bulk.

Additional information from the extended hydrophobic/water interface has been obtained by X-ray[206,207,208,209] and neutron reflectivity.[210,211] These techniques are sensitive to the electron and scattering length density, respectively, and can be used, in principle, to determine water density profiles from the interface. Similarly to VSFS, the preferred model system has been alkylsilane terminated monolayers, self-assembled on silicon dioxide surfaces. One important result that has emerged from these studies is evidence supporting the presence of a density depletion layer next to the hydrophobic surface. The actual

thickness of this gap remains a source of debate, but the latest consensus suggests that for alkyl silane monolayers it is in the order of 1.5 Å or less,[207,209,212,213] that is, just a fraction of a water monolayer (note that when considering error bars the possibility of having no gap at all is also an option in many studies). Besides the difficulties associated with preparing defect-free silane monolayers of sufficiently good quality described previously for VSFS,[197,200] the other factors contributing to the uncertainty in the gap determination are linked to limitations in the instrument resolution, which are more patent in neutron reflectivity.[209,213] Recent confirmation of the presence of an interfacial depletion layer comes for example from X-ray reflectivity (XRR) on perfluorinated self-assembled monolayers of varying fluorocarbon chain length (see Figure 13).[212] Defect-free fluorocarbon self-assembled monolayers are more difficult to prepare than equivalent alkylsilane monolayers.[214,215] However, their increased hydrophobicity enhances, in principle, the gap width relative to the resolution limit.

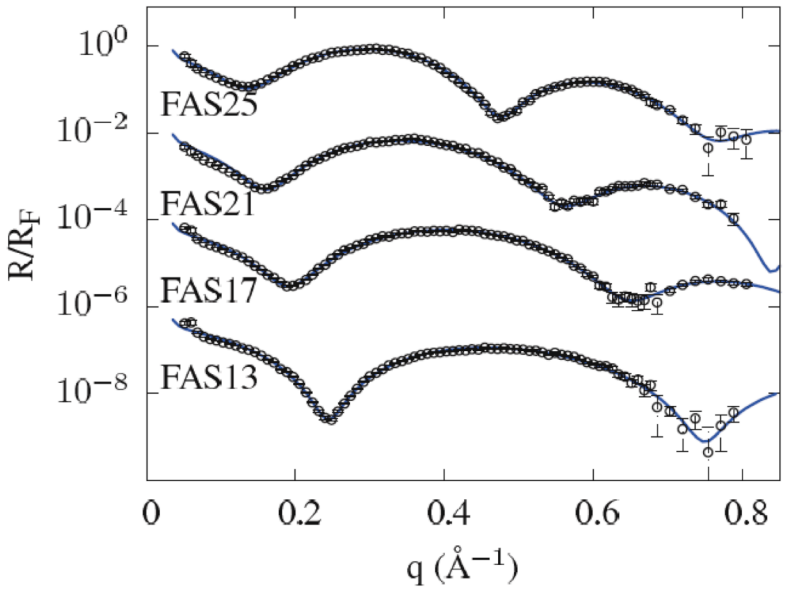

Figure 13. X-ray reflectivity data for a series of fluoralkylsilane monolayers, $CF_3(CF_2)_n(CH_2)_2SiCl_3$, with varying lengths of CF_2 groups in contact with water. For FAS13, FAS17, FAS21, and FAS25 the values of "n" is equal to 5, 7, 9, and 11, respectively. Fits to the spectra are shown as solid lines. Unambiguous gaps with minimum confidence errors of just a fraction of an Å are only observed for the longer chain monolayers (FAS21 and FAS25). Reproduced from reference 212.

A comparison of the XRR and VSFS results suggests that the apparent density depletion layer is linked to water molecules with a dangling OH bond in direct contact with the hydrophobic surface. Nonetheless, the VSFS spectra clearly indicate that those dangling OHs, as well as the terminal methyl groups of the alkyl silane monolayer, are vibrating in neither vacuum nor air. This is confirmed by the red shift of ~25 cm^{-1} and ~3 cm^{-1}, relative to when in contact with air, for the "free OH" and CH_3 stretching modes, respectively.[196,197,200] It is worth mentioning, however, that in perfluoroalkylsilane monolayers the relative shift for the OH dangling mode is limited to just ~10 cm^{-1}.[197]

We will close this section with a few words on the molecular structure of water next to fluid model hydrophobic interfaces, such as oil/water interfaces, where available information is much more limited compared to the case of solid hydrophobic interfaces. Investigating liquid hydrophobic interfaces has been hampered by experimental challenges.[216] Nevertheless, planar fluid interfaces, including water/CCl_4[198] and water/alkane[196,198,217] systems have been investigated using VSFS. In all cases and similarly to the alkylsilane monolayer systems, water molecules with dangling OHs have been detected. The extent of ordering of water molecules beyond the first monolayer remains, however, uncertain due to conflicting reports, where the purity of the oils used may play a significant role in the interpretation of the results.[198,217] Interestingly, careful ellipsometric studies at a series of planar oil/water interfaces have provided support for a depletion layer of just a fraction of an Å (0.3-0.4 Å).[218] These reported values are close to those expected simply from hard sphere repulsion. The calculate thickness for the gap, remain however, model dependent.

The results obtained for planar oil/water interface may not necessarily extend to curved interfaces, even if the radius of curvature is large relative to molecular scales. A recent vibrational sum frequency scattering study on alkane/water nanodroplets (~275 nm in diameter), reports that non-dangling OH bonds are observed at such interfaces.[219] Even if not yet confirmed by others, it is clear that a number of open questions remain regarding the surface structure of water next to hydrophobic surfaces.

6. LIQUID/VAPOR INTERFACES

In this section we will discuss the interface of liquid water and aqueous solutions with vapor. This interface represents a termination of the hydrogen-bonding pattern of liquid water. Water molecules at the very surface will on average have a reduced number of hydrogen bonds compared to those in bulk liquid water. For pure water, this results in various surface-specific phenomena, as discussed in Ref. 220. We will in this chapter focus on surfaces of aqueous solutions, which are highly relevant in environmental sciences and as models for hydrophobic interfaces. In atmospheric science, the role of the liquid-vapor interface is an important but insufficiently understood factor for climate change.[221] In particular, due to their high surface-to-bulk ratios, the properties of atmospheric aerosols are strongly influenced by interfacial molecular-scale phenomena. Moreover, the vapor phase above the aqueous surface effectively acts as a very hydrophobic surface, making the liquid-vapor interface a useful model for hydrophobic interfaces, which were discussed in the previous section.

A key issue in these contexts is how the composition of the surface of a solution differs from that of the bulk. Some idealized cases are schematically illustrated in Fig. 14. While solutes are homogeneously

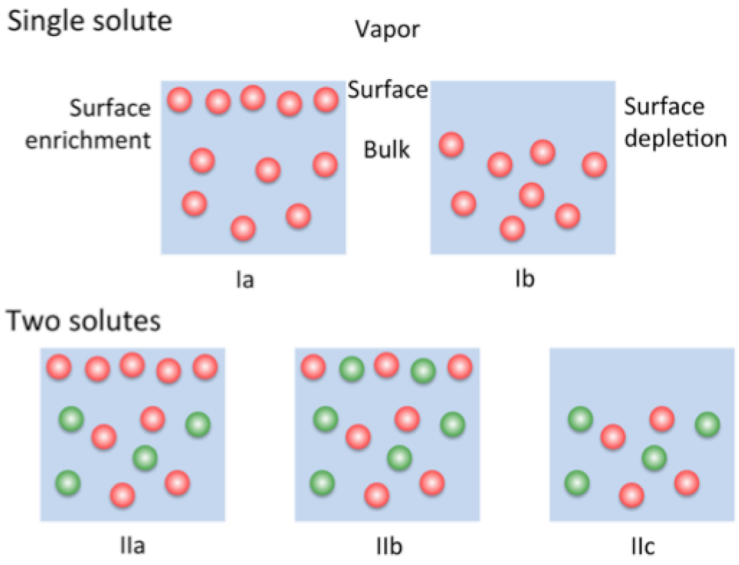

Figure 14. Schematic illustration of how the composition of the surface of a solution may differ from that of the bulk for a solution with a single solute (Ia and b) or two solutes (IIa, b and c).

distributed in the bulk of a solution, the spatial distribution of solutes in the surface-near region is often different. While some solutes are enriched at the surface (Fig. 14 Ia), others are instead depleted (Fig. 14 Ib). In solutions with two or more solutes, the distribution of the solutes close to the surface may be independent from each other and add up to the sum of the single solute cases. For example, a mixture of two surface-depleted species, each with a distribution as in Fig. 14 Ib, would result in a spatial distribution like the one in Fig. 14 IIc, while a mixture of two surface enriched species, each with a distribution as in Fig. 14 Ia, would be spatially distributed such as depicted in Fig. 14 IIb.

Due to effects such as differences in solvation energy, leading to competition for solvating water molecules, and inter-solute interactions, such as complex formation or ion-pair formation, the spatial distribution of the solutes at the interface may, however, be different from the sum of the two separate cases. The addition of a second solute may cause a species, which is surface enriched on its own as in Fig. 14 Ia, to avoid the surface as shown in Fig. 14 IIc. An independently surface depleted species, as in Fig. 14 Ib, may become surface enriched due to the addition of a second species as in Fig. 14 IIa. In the case of a mixture of two independently surface enriched species, each with a distribution as in Fig. 14 Ia, the result may be that one of the two solutes dominates the surface region as in Fig. 14 IIa. Some selected results from literature, which demonstrate those general examples, are described below.

6.1 Methods

To probe the surface of water and aqueous solutions various surface sensitive and selective experimental techniques are established, mainly vibrational sum-frequency spectroscopy (VSFS)[222,223], second harmonic generation (SHG)[224] and X-ray photoelectron spectroscopy (XPS) on liquid micro jets[225] and on deliquescent salt crystals[5]. Furthermore, other techniques such as X-ray and neutron scattering[226], and various X-ray based experimental methods such as grazing incidence X-ray diffraction, X-ray reflectivity and total reflection X-ray fluorescence[227] are used to study monolayers of amphiphilic molecules on the aqueous surface. VSFS and SHG allow for deduction of structural information on composition and orientational distributions from vibrational modes. In XPS, where chemical compounds

are monitored directly, chemical and structural information as well as spatial distributions of species are revealed by means of detection of photoelectrons. The surface sensitivity in the non-linear optical techniques (VSFS and SHG) relies on a disruption in inversion symmetry at the interface, and in XPS surface sensitivity is obtained by a short attenuation length of the emitted photoelectrons in the condensed phase. Inaccuracies in the quantification of the spatial distributions of ions and molecules at the aqueous surface arise in VSFS and SHG from the fact that the position where the symmetry breaks changes for various solutions and in XPS from the fact that the attenuation lengths of photoelectrons in water in dependence on their kinetic energies are in particular for lower kinetic energies not exactly determined. Both VSFS and XPS experiments can be performed at ambient conditions. In liquid-micro jet experiments the solution surface is continuously renewed, which avoids problems due to beam damage in XPS experiments. In contrast to that is the preparation of a contamination-free surface in static samples, like it is used in e.g. SFG experiments, extremely challenging. Information about the aqueous surface on the microscopic scale can also be obtained by Molecular Dynamics simulations.[228,229,230] These provide detailed information about the spatial distributions of different species at the surface. The accuracy of the simulations depend critically on the quality of the used force fields, and the results are also influenced by the limited size of the systems possible to simulate.

6.2 Structure and chemical composition of the aqueous interface: Pure water

From VSFS studies on the structure of the pure aqueous interface, there seems to be common agreement that a single OH group projects into the vapor phase free of hydrogen bonding (*i.e.*, a hydrogen dangling bond), which corresponds to a peak at 3700 cm^{-1}.[222] We note that this peak is blue-shifted by 20 cm^{-1} when compared to methyl terminated solid hydrophobic/ water interfaces discussed above). In the past the peak around 3200 cm^{-1} has been assigned to an "ice-like" structure, *i.e.* tetrahedral and strongly bonded water molecules, while the one around 3450 cm^{-1} was attributed to more disordered water. However, more recent studies indicate that these peaks are due to a mixing of the bending overtone modes in water with the stretching motions causing Fermi resonance and splitting the band into two peaks.[231]

Regarding the acid/base characteristics of the aqueous interface there are contradictory statements. There is a discrepancy in experimental results and in theoretical predictions from simulations regarding the spatial distribution of protons (and structure/hydration: e.g. Eigen and Zundel) and hydroxide ion at the aqueous interface.[224,228,232] The structure of the aqueous interface, as well as its acid/base characteristics, is discussed in more detail in Ref. 220.

6.3 Structure and chemical composition of the aqueous interface: Solutions

Many of the fundamental processes of biological, environmental and atmospherically relevance occur at the water-vapor interface, however the understanding of the behavior of ions, organic and inorganic molecules at the interface is still under development. Most studies conducted on the aqueous interface during the last decades, show a clear difference in the chemical composition at the interface in comparison to the bulk.

6.3.1 Salts

Many efforts have been expended on giving simple rules on how various compounds behave at the aqueous surface, however strong controversial claims give rise to discussions. The common consensus seems to be that simple rules are difficult to state. However, trends for classes of compounds, such as halides or organic molecules can be given. Small inorganic ions, such as halides, are classically expected to be depleted from the surface, see Fig. 14, Ib, in part due to the lack of polarizable solvent outside the air-water interface.[233] It is, however, largely agreed on in the community that big, polarizable halide anions are less depleted from the surface in comparison to smaller, less polarizable ions, and that iodide may even be enriched (Fig 14, Ia). Nevertheless, their quantitative enhancement, determined both experimentally and theoretically, is discussed and there is considerable disagreement on quantitative values.[234,235,236,237] Besides the studies on pure halide salts, mixtures of various inorganic salts in aqueous solutions have been investigated throughout the years and cooperative effects were found.[238] Depending on the exact mixture, the interaction between ions may be driven by various energetic and entropic effects

resulting in e.g. ion pairing and/or segregation of one species at the water vapor interface. Furthermore, close to the interface region less water is available for hydration of the compounds. At elevated salt concentrations / ionic strength this fact leads to competition for full hydration among the different dissolved ions. This may favor ion pairing such as solvent-separated ion pairs, contact ions pairs and complex formation at the interface[239], all of which are effects that are rather unexplored.[240,241] Another issue is the interaction between ions and molecules[242,243] as well as molecules and molecules, which are also in the scope of numerous investigations and are discussed in more detail in the following section.

6.3.2 Molecules

In contrast to inorganic ions, which can exhibit either surface enrichment or depletion, organic molecules are often enriched at the interface causing a decrease in surface tension. Already rather small organic compounds that are freely miscible in water can be enriched at the aqueous surface, *i.e.* the surface concentration is in general larger than the bulk concentration. As a result of this surface enrichment in particular surfactants, *i.e.*, surface-active amphiphilic molecules, can show orientation effects at the aqueous interface which are most often driven by minimization of hydrophilic-hydrophobic interactions and an increase in van der Waals interactions between hydrophobic parts of the molecules.[244] A known example in this context is that alkyl-chains of organic molecules or ions can be oriented perpendicular to the water surface plane at monolayer coverages.[244,245,246] Thus the interfacial structure of a solution can be strongly altered depending on the solutes. For certain compounds (*i.e.*, acetic acid, methanol, acetone) even the formation of centrosymmetric or antiparallel double layer structures at the surface has been observed at elevated concentrations.[247,248,249,250]

In mixtures of molecules and inorganic salts in aqueous solutions, different cooperative effects have been observed which affect, e.g., the concentration and structure of solutes at the aqueous interface. In this context, terms such as “salting out” and “salting in” were established by F. Hofmeister[251], based on experiments on mixtures of inorganic ions and proteins. This effect of cations and anions on the solubility of organic compounds, which is caused by direct and indirect interactions between the solutes, has also

been observed for various other amphiphilic organic molecules affecting their behavior close to the interface (Ref. 252 and references therein). Some experiments show for example evidence for direct interaction between the organic compounds and the dissolved ions, which effectively can change the spatial distribution and orientation of the solutes at the aqueous interface. [242,253]

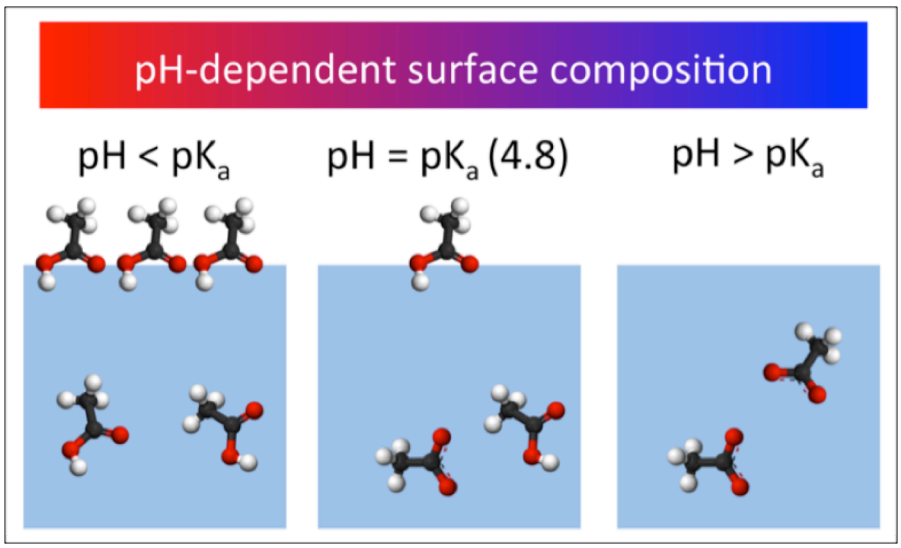

Figure 15. A schematic illustration of the differences in composition between the surface and bulk of aqueous acetic acid as function of pH.

As discussed in Ref. 220, the pure water surface may be different from the bulk in terms of hydroxide and hydronium ions. Connected to this is the behavior of an acid or base at the aqueous surface, which has been studied for example by XPS.[254,255,256] The results for acetic acid are schematically shown in Fig. 15. Assuming equal activities, the protonated and deprotonated forms exist with the same concentration in the bulk at a pH equal to the bulk pK_a, *i.e.* 4.8. At the surface, however, the protonated species dominates. At pH << pK_a, the bulk is dominated by the protonated species, which furthermore is surface enriched. At pH >> pK_a, the deprotonated species dominates the bulk, and very little of either species is found at the surface. The surface composition is thus different from the bulk composition in terms of both the solute amount and speciation. Similar behavior has also been observed for other acids.[247,254,255] There are, however, other aspects on the surface behavior of acids. Mass-spectroscopic studies of hexanoic acid /

water droplets suggest that the deprotonation of the acid can occur at the surface down to pH well below the bulk pK_a, interpreted as caused by the presence of hydroxide ions at the surface at pH down to 4.[232] There are several factors that may influence the speciation of an acid/base at the water surface, such as the possible prevalence of either hydronium or hydroxide ions, the possible change of the pK_W at the surface, and surface segregation phenomena of both the protonated and deprotonated species.

6.4 Open issues

As briefly mentioned above, there are a number of open issues connected to the liquid-vapor interface. For neat water, there are issues such as the number of dangling OH-groups, and the possibly different pK_W and pH. Regarding aqueous solutions of molecules and ions, a precise determination of the spatial distribution of different species at the aqueous interfaces and connected effects, such as possible double-layer formations, orientational or cooperative effects, is both of strong fundamental interest and highly relevant in, e.g., atmospheric science. Single solute systems are now actively studied, and the understanding of such relatively simple systems is a necessary prerequisite to proceed to more complex systems closer to those found in nature, such as mixtures of two or more solute species. How the presence of solutes at the surface influences the adsorption of water molecules from the vapor phase, a key process in water accommodation in the atmosphere, has only been begun to be explored. All these effects can be expected to exhibit a temperature dependence, which remains to be studied in more detail.

On the methodological side, both experimental and theoretical methods employed to study the aqueous surface on the molecular scale have unsolved challenges requiring certain assumptions to be made when results are analyzed and interpreted. Thus, results need to be treated with caution and often only qualitative trends can be concluded. Hence, there is a need to specify insufficiently determined parameters even more in order to improve the accuracy of the results. For example the attenuation length of electrons in aqueous matter, which is a measure of the surface sensitivity of XPS is not known accurately.

Molecular dynamic models are strongly dependent on the employed force fields, while ab initio quantum chemical simulations, which are computationally more expensive, can only be applied to smaller systems and are still not exact, suffering from errors in the treatment of e.g. van der Waals forces (as mentioned earlier) and self-interaction (which is particularly relevant to the acid/base properties of pure water)[257,258]. Thus results from these studies can at best give trends, while the precise determination of e.g. the spatial distribution of compounds at the interface and connected effects is still very challenging. Our understanding of the liquid-vapor interface is now rapidly developing, and further progress on issues of both fundamental interest and applied relevance can be expected from established experimental and theoretical techniques, and especially combinations thereof, and possibly new techniques.

7. ICE/VAPOR INTERFACES

Like most solids, ice undergoes a melting transition at the solid/vapor interface at temperatures below the bulk melting point.[259,260] As such, the ice surface can essentially change its nature from that of a solid/vapor to a liquid/vapor interface, depending on the temperature. The existence of a disordered, liquid-like layer (LLL; sometimes also called "quasi liquid-like") has consequences for, e.g., the friction and adhesion of ice surfaces, the adsorption, reaction and release of trace gases from the ice surface, and is also a key component in models for the mechanism leading to thundercloud electrification. The existence of a LLL at the ice surface was first proposed by Michael Faraday in 1859, based on observations of a growing contact area between two ice spheres in contact with each other, which Faraday interpreted as a sign for the presence of a mobile layer at the ice surface.[261] Experimental proof for the existence of the LLL on the ice surface proved to be elusive for a long time; only in the last decade of the past century did several surface-sensitive techniques show that the ice surface indeed exhibits a premelting transition. However, the nature of the LLL is far from being understood - there is not even agreement on its two most fundamental characteristics, namely the onset temperature for surface melting and the thickness of the LLL as a function of temperature. There is even less information on other important parameters, such as the density of the LLL, its viscosity, and its ionic and electric conductivity, and whether there is a sharp boundary between the LLL and the solid ice, or rather a gradual transition.

7.1 Thickness of the liquid-like layer

The onset temperature and thickness of the LLL have been studied using a variety of techniques, including proton channeling, grazing incidence X-ray diffraction, SFG, AFM, ellipsometry, and NEXAFS. A compilation of the results of these measurements is shown in Fig. 16.[8] The thickness of the LLL varies by up to two orders of magnitude for a given temperature, depending on the measurement. These large discrepancies are most likely due to two factors. For one, different techniques measures different physical properties to distinguish liquid water from solid ice, e.g. X-ray diffraction the disorder in the O lattice positions, ellipsometry a change in the complex refractive index, and AFM the adhesion

force between the tip and the ice surface. With the uncertainty in the properties of the liquid layer this can lead to variations in the results. A second possible reason for the large uncertainties is the role of impurities in the surface melting of ice, which may alter the onset temperature for premelting.[262,263,264,265,266]

A surface science approach to the study of the physical and chemical properties of the ice surface requires the preparation of well-ordered single crystal surfaces as well as the control of impurities in the experiments. Each one of these conditions has been fulfilled during the last decade, yet not in one-and-

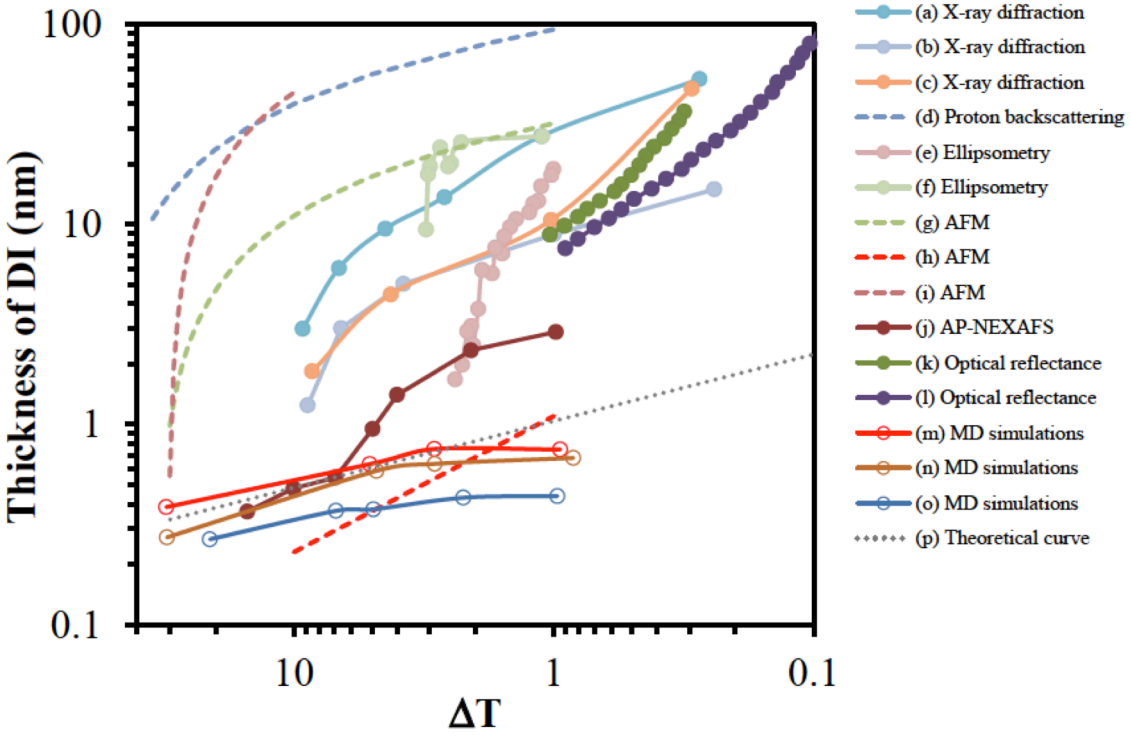

Figure 16: Thickness of the liquid-like layer as a function of temperature, as determined using various experimental and theoretical methods. Reproduced with permission from Ref. 8.

the-same experiment. Dosch et al. have conducted ground-breaking glancing angle X-ray scattering experiments on carefully-prepared hexagonal (00.1) and non-basal (10.0) and (11.0) ice I*h* surfaces, where X-rays with a photon energy of ~8.3 keV where incident on the surface at an angle of total external reflection, about 0.14 deg to the plane of the surface.[267,268] Under these conditions the probing depth in the experiments can be varied from ~5 nm to ~100 nm by slight variations of the angle of incidence. The

extreme grazing incidence angle required the preparation and the maintenance of very smooth and extended surfaces. By monitoring both the X-ray reflections due to the oxygen atoms in the ice lattice and the hydrogen-forbidden (00.4) reflections, these studies yielded information about the disorder in the water molecule positions as well as the disruptions in the hydrogen-bonded network due to Bjerrum defects. The glancing X-ray scattering experiments revealed an onset temperature for premelting of -13.5 C for the basal and -12.5 C for the non-basal surfaces, with LLL thicknesses of 30 nm and 10 nm at -1 C for the basal and non-basal surfaces, respectively. These data are in good agreement with a thermodynamic model based on a minimization of the interfacial free energy through lattice calculations in the grand canonical ensemble by Henson et al.[269] They are also consistent with coarse-grained free energetic modeling and molecular simulations of a minimal model of water.[270]

A number of ab initio simulations of the ice surface and classical MD simulations of melting at the ice surface have been performed to understand various molecular level aspects of the ice/vapor interface.[271,272,273,274,275,276,277,278,279,280,281,282,283] For example, ab initio simulations have focused on understanding how protons in the hydrogen bonded network of ice order at the surface and how this ordering impacts upon adsorption and pitting at the surface.[277,283] Classical MD simulations have focused on the formation of the LLL, and in this regard it is encouraging that they do consistently predict the formation a LLL below the melting temperature of ice and that it increases in thickness as the temperature approaches the melting temperature (or more precisely the water model used). Fig. 17 shows an example of one such classical MD simulation for an ice nanoparticle. It shows that at >30 K below the melting temperature of the nanoparticle there is some configurational disorder of the water molecules at its surfaces but no clear LLL. In contrast at just a couple degrees below the melting temperature of the nanoparticle a ca. nanometer thick LLL is apparent. The particular study from which Fig. 17 was extracted also explored where in the nanoparticle pre-melting was favored, revealing that it was initiated at the corners of the crystals, then the edges between facets, and finally at the flat surfaces, *i.e.*, the melting temperature is related to the degree of coordination. A strong dependence of the melting temperature with the nanoparticle size was also observed, with the combination of small particle size and

pre-melting leading nano-sized ice crystals to have liquid-like surfaces as low as about 130 K below the bulk ice melting temperature.

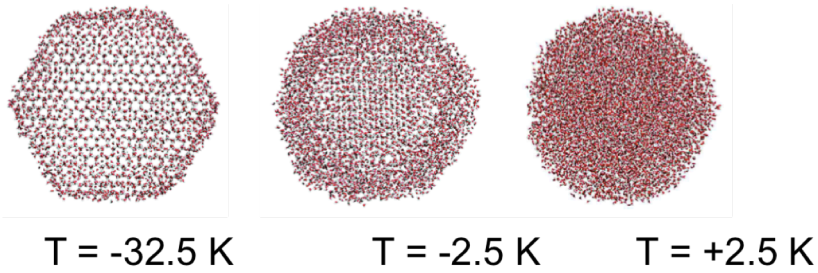

Figure 17. Snapshots from classical MD simulations of an ice nanocrystal as a function of temperature (relative to the melting temperature of the nanoparticle with a particular classical model). At low temperatures (left image) there is some configurational disorder at the ice surface but no significant LLL. At just a couple of degrees below the melting temperature (middle image) a clear LLL has emerged. This particular nanoparticle contains about 10,000 water molecules. Image adapted from Ref. 280.

7.2 Reaction of ice with adsorbates

One unsolved problem in these experiments is the presence of surface contamination, which are in general not easily to detect using X-ray scattering. Impurities at the ice surface may originate from adsorption from the surrounding gas atmosphere, or from the bulk itself, where even small amounts of impurities in the stock solution from which the ice is grown can give rise to considerable amounts of impurities at the surface. A promising method for the simultaneous measurement of the surface chemical composition and surface disorder of ice is a combination of ambient pressure X-ray photoelectron spectroscopy (APXPS) and near-edge X-ray absorption fine structure (NEXAFS) at the oxygen K-edge. NEXAFS probes unoccupied orbitals and is sensitive to the local bonding environment, for instance to changes in the hydrogen bonding between water molecules. When operated in the partial electron yield mode, with a probing depth of about several nm, it allows probing the degree of disorder at the ice surface. Using this approach an onset temperature of about –20 °C for the premelting of a polycrystalline ice sample was found[266], in reasonable agreement with the grazing incidence X-ray scattering experiments

shown above. These measurements also indicated that adventitious carbon contamination from the vacuum chamber background enhances premelting.

Over the recent years several combined APXPS/NEXAFS studies have addressed the influence of contamination on the premelting of ice. An illustrative example is shown in Fig. 18, where an initially clean ice surface was exposed to increasing partial pressures of NO_2, and important trace gas in the atmosphere.[284] The experiments were performed at -43 °C. XPS and Nitrogen K-edge NEXAFS both showed the formation of nitrate species at the ice surface through the reaction of NO_2 with water. The left panel in Fig. 18 presents the O K-edge NEXAFS spectra for the clean ice (blue line), a submonolayer coverage of nitrate on the ice surface formed at a NO_2 partial pressure of 0.003 Torr (green points), and a spectrum of a nitrate solution droplet which formed at a NO_2 partial pressure of 0.05 Torr. The peak at ~532 eV is due to oxygen in the nitrate.[285] The transition from solid ice to a nitric acid solution is visible through the characteristic increase in the intensity of the peak at 535 eV (see earlier section) and the increase in the main edge intensity (~537 eV) over that of the post edge (~542 eV) for the solution compared to the ice. The right panel in Figure 18 shows the results of a linear compilation of the pure ice

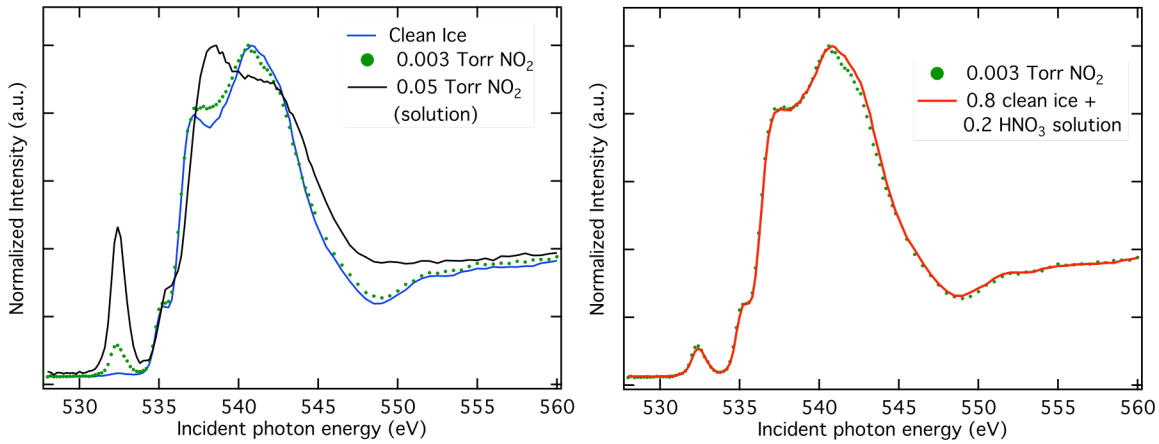

Figure 18. Effect of the presence of a submonolayer of HNO_3 on the ice surface at 230 K. The NEXAFS data of the HNO_3 covered ice (green dots) can be approximated in a linear combination of the O-K edge NEXAFS spectrum of clean ice (blue line) and a HNO_3 solution (black line) in a ration of 0.8:0.2 (see right panel). These data indicate that the disordered layer at the ice surface in the presence of a submonolayer coverage of HNO_3 is due to an HNO_3 solution, instead of a premelted ice layer. From Reprinted with permission from Ref. 284.

with the pure solution spectrum to fit the spectrum obtained for sub-monolayer nitrate coverage. The best fit is achieved with 0.8 clean ice + 0.2 nitric acid solution, which would be consistent with a coexistence of the two components without additional premelting induced by the presence of nitric acid. Other experiments of ice/adsorbate interfaces have been performed with acetone[286], acetic acid[287] and 2-propanol.[288]

While this is an important step forward in our understanding of the influence of impurity phases on the nature of the ice surface, many more measurements spanning range from stratospheric temperatures to the melting point, and impurities, including alkali halides, acids and organics, are necessary to provide much needed input data for models of the heterogeneous chemistry of polar snow packs and ice aerosol particles in the atmosphere. An ideal experiment would combine simultaneous measurements using surface sensitive X-ray crystallography (such as gracing incidence X-ray scattering) and XPS which would provide structural as well as chemical information on the surface. With the advent of dual hard/soft X-ray beamlines this might not be too far-fetched a dream.

8. CONCLUDING REMARKS

If one would attempt to sort aqueous interfaces by the degree of molecular-level understanding we have gained through theoretical and experimental studies over the past decades, the solid/vapor interface would surely rank highest, in particular in view of the wealth of information gleaned from experimental studies at low-temperature conditions and theoretical modeling of water adsorption on well-ordered substrates. Structural motifs, hydrogen-bonding between water molecules, dissociative vs. molecular adsorption, and the kinetics of water molecule migration along the interface have been explored with a range of theoretical and experimental methods. Much less is known about the interfaces of bulk aqueous solutions at ambient temperatures, e.g., the bulk liquid/vapor and liquid/solid interface, which in the case of aqueous solutions in general show deviations in the chemical composition compared to that of the bulk, and where the hydrogen bonding network may deviate from that in the bulk due to the presence of the interface. The highly dynamic nature of these interfaces at ambient temperatures poses challenges to both

experimental and theoretical investigations. While we have made progress in the molecular-scale description of the steady-state properties of liquid/solid as well as liquid/vapor interfaces over the last years, a detailed understanding of heterogeneous processes at aqueous interfaces is still a major challenge and requires new experimental and theoretical approaches. Progress in this area will have a strong impact across many diverse areas of science and technology, including such important phenomena as the uptake of CO_2 at the ocean surface, and the fundamental processes involved in electrochemical reactions, such as corrosion, in particular simultaneous charge and mass transport.

AUTHOR INFORMATION

Corresponding Author

*E-mail: hbluhm@lbl.gov

Notes

The authors declare no competing financial interest.

Biographies

Olle Björneholm is a Professor of Physics at the Department of Physics and Astronomy at Uppsala University. He obtained his Ph.D. in physics from the Uppsala University in 1992 on studies of adsorbed molecules, after which he studied free clusters as a postdoctoral researcher at Hasylab at DESY in Hamburg. He now leads a research group at Uppsala University studying aqueous interfaces, with special emphasis on the liquid/vapor interface in connection to atmospheric science.

Martin H. Hansen is a PhD student with the Center for Atomic-scale Materials Design at the Department of Physics, the Technical University of Denmark (DTU). He obtained his Master degree in Physics and Nanotechnology from DTU in 2013 under supervision of Prof. Jan Rossmeisl, with whom he has continued to work during the PhD. His research is focused on electro-catalysis and new methods for modeling electrolyte-electrode interfaces with density functional theory.

Andrew Hodgson s a member of the Surface Science Research Centre and Head of the Department of Chemistry at Liverpool University. He did his PhD (University of London) in the field of gas phase reactions and laser spectroscopy, his post-doctoral research (University of Nottingham) on photochemistry of small molecules before gaining an EPSRC Fellowship and moving to University of Liverpool in 1986. At Liverpool his research has focused on reaction dynamics at solid surfaces, with an increasing interest in ice surfaces and the water-metal interface.

Li-Min Liu received his PhD degree in Materials Science from the Institute of Metal Research, Chinese Academy of Sciences, in 2006. During his PhD study, he visited Queen' University of Belfast, U.K., for a year. Then he worked in Fritz-Haber-Institut, University College London, and Princeton University. Since 2012, he takes a tenure-track position in Beijing Computational Science Research Center. He has co-authored more than 100 journal papers. He was granted "1000-plan for the young talent" and "the National Science Fund for Excellent Young Scholars". His research interests focus on the nanocatalysts, TiO_2-based photocatalysis, and aqueous water solid interfaces for the electrocatalysis and full cell.

David T. Limmer received his Ph.D. in chemistry at the University of California, Berkeley, in 2013, working with David Chandler. Currently, Limmer is a research fellow at the Princeton Center for Theoretical Science at Princeton University where his research interests include developing modern statistical mechanical descriptions of interfacial phenomena and condensed phase dynamics. In the summer of 2016, he will join the faculty University of California, Berkeley as the Chevron Chair in Chemistry, and Heising-Simons Fellow at the Kavli Energy NanoSciences Institute.

Angelos Michaelides obtained a Ph.D. in Theoretical Chemistry in 2000 from The Queen's University of Belfast. Following this he worked as a post-doctoral research associate and junior research fellow at the University of Cambridge and then at the Fritz Haber Institute, Berlin, as an Alexander von Humboldt research fellow. Subsequently he was promoted to staff scientist and research group leader at the Fritz Haber Institute. In 2006 he moved to University College London, where since 2009 he has been Professor of Theoretical Chemistry. Research in his group (www.chem.ucl.ac.uk/ice) involves computer simulations of catalytic and environmental interfaces, aiming at reaching fundamental new understanding of elementary processes at such interfaces. Water is a major focus of their work.

Philipp Pedevilla obtained his MSc. from Leopold Franzens University of Innsbruck (Austria) in 2013. He is currently working towards obtaining his PhD degree at University Colllege London in the group of Prof. Angelos Michaelides. His interests are ab initio and classical force field simulations of aqueous interfaces.

Jan Rossmeisl is a Professor of Theoretical Chemistry at the Department of Chemistry and the Nano-Science center at Copenhagen University. Before joining the University of Copenhagen in April 2015, Jan was an Associate Professor and group leader for the Theoretical Catalysis group at the Department of Physics at the Technical University of Denmark. Jan holds Master's (2000) and Ph.D (2004) degrees in physics from the Technical University of Denmark. Since 2007 he has supervised more than 20 Ph.D students and postdocs. He is an author or coauthor of more than 110 publications in peer reviewed journals, a co-inventor of 4 patents, and a co-founder of two startup companies. His research interests include electrocatalysis, energy conversion, atomic scale simulations, and rational interface design for catalysis.

Huaze Shen is a PhD student in International Center for Quantum Materials, Peking University, China, under the supervision of Prof. Enge Wang and Prof. Limei Xu. He obtained his B.Sc.degree in Physics in 2012 from Sichuan University, China. His research is now focused on the theory and simulation of nucleation mechanism of clathrate hydrates in liquid solutions, especially near the liquid/solid interfaces.

Gabriele Tocci obtained his B.Eng. in Energy Engineering from Sapienza University of Rome (Italy) in 2008 and his M.Sci. in Nanotechnology from Kungliga Tekniska Högskolan (Sweden) in 2010. Following this, he undertook a P.hD. in Theoretical Chemistry under the supervision of Prof. Angelos Michaelides at University College London. After being awarded his Ph.D. in 2014 he has moved to the École polytechnique fédérale de Lausanne (Switzerland), where he has been working as a post-doctoral research associate. His interests are in the ab initio modeling of aqueous interfaces and in the atomistic simulations of non-linear light scattering in aqueous solutions.

Eric Tyrode is an Associate Professor in Physical Chemistry at the Department of Chemistry at KTH Royal Institute of Technology in Stockholm. Chemical Engineer by training (University of the Andes, Venezuela), he holds a PhD in Chemistry (2005) from KTH. After postdocs in Hokkaido University (Japan) and Durham University (UK), he moved back to Sweden in 2008. His research focuses on understanding molecular structure at aqueous interfaces, primarily by making use of surface-specific linear and non-linear optical techniques. Tyrode is recent recipient of the SSF Future Research Leader award.

Marie-Madeleine Waltz is a researcher at the Department of Cell and Molecular Biology in the division for Computational and Systems Biology at Uppsala University. She received her M.Sc. in Molecular Science (2008) and her Ph.D. in physical chemistry (2012) from the University Erlangen-Nuremberg (Germany). From 2013 to 2014, she worked as a postdoc at the Department of Physics and Astronomy in the division for Molecular and Condensed Matter Physics at the Uppsala University (Sweden) by means of a stipendium from the Carl Tryggers foundation. Her research interests cover experimental studies using spectroscopy and microscopy in the field of surface science with focus on interfacial processes of aqueous solutions and solids, as well as Molecular Dynamics simulations. She received the Women's faculty award from the University Erlangen-Nuremberg, Germany.

Josephina Werner is a PhD student in the Department of Physics and Astronomy at Uppsala University (UU) and in the Department of Chemistry and Biotechnology at the Swedish University of Agricultural Sciences (SLU), Uppsala (Sweden). She obtained her M.Sc. in atomic and molecular physics from the University of Giessen (Germany) in May 2011. Since July 2011, she is working in Uppsala under the joint supervision of Prof. Olle Björneholm (UU) and Prof. Ingmar Persson (SLU). Her research focuses on aqueous and nanoparticle surfaces studied mainly by X-ray-based spectroscopy methods.

Hendrik Bluhm is a Senior Scientist in the Chemical Sciences Division at Lawrence Berkeley National Laboratory and an Adjunct Professor in the Department of Chemistry&Biochemsitry at the University of Maryland, College Park.. He obtained his M.Sc. in Crystallography from the University of Leipzig (Germany) and his Ph.D. in Physics from the University of Hamburg (Germany). After a postdoc at LBNL he joined the Fritz Haber Institute of the Max Planck Society in Berlin, before moving back to LBNL and his current position. His research focuses on the interfacial chemistry of surfaces (e.g., metal oxides, ice, and aqueous solutions) under relevant environmental conditions, as well as the development of new experimental methods for the investigation of interfaces under operating conditions. Bluhm is a AAAS Fellow and a recent recipient of a Bessel Award from the Alexander von Humboldt Foundation.

Acknowledgements

This review was initiated during the Nordita (Nordic Institute for Theoretical Physics) scientific program "Water - the Most Anomalous Liquid". Additional financial support for this program was provided by the Royal Swedish Academy of Sciences through its Nobel Institutes for Physics and Chemistry, by the Swedish Research Council and by the Department of Physics at Stockholm University. H.B. acknowledges support by Director, Office of Science, Office of Basic Energy Sciences, and by the Division of Chemical Sciences, Geosciences, and Biosciences of the U.S. Department of Energy at LBNL

under Contract No. DE-AC02-05CH11231. A.M. and P.P's work is supported by the European Research Council under the European Union's Seventh Framework Programme (FP/2007-2013)/ERC Grant Agreement No. 616121 (HeteroIce project). A.M. is also supported by the Royal Society through a Wolfson Research Merit Award (A. M.). E.T. acknowledges support from the Swedish Research Council (VR) and the Swedish Foundation for Strategic Research (SSF- Future Research Leaders program). Financial support from the Carl Tryggers foundation is gratefully acknowledged (M.-M. W.).

References

[1] Carpenter, L.J.; Nightingale, P.D. *Chem. Rev.* **2015**, *115*, 4015.

[2] Gileadi, E. *Physical Electrochemistry*, Wiley VCH, Weinheim, 2013.

[3] Zaera, F. *Chem. Rev.* **2012**, *112*, 2920.

[4] Zaera, F. *Surf. Sci.* **2011**, *605,* 1141–1145.

[5] Krisch, M.J.; D'Auria, R.; Brown, M.A.; Tobias, D.J.; Hemminger, J.C. *J. Phys. Chem. C* **2007**, *111*, 13497.

[6] Davies, J.F.; Miles, R.E.H.; Haddrell, A.E.; Reid, J.P. *PNAS* **2013**, *110*, 8807.

[7] Jungwirth, P.; Tobias, D. J. *Chem. Rev.* **2006**, *106*, 1259.

[8] Bartels-Rausch, T; Jacobi, H.-W.; Kahan, T.F.; Thomas, J.L.; Thomson, E.S.; Abbatt, J.P.D.; Ammann, M.; Blackford, J.R.; Bluhm, H.; Boxe, C.; Domine, F.; Frey, M.M.; Gladich, I.; Guzmán, M.I.; Heger, D.; Huthwelker, Th.; Klán, P.; Kuhs, W.F.; Kuo, M.H.; Maus, S.; Moussa, S.G.; McNeill, V.F.; Newberg, J.T.; Pettersson, J.B.C.; Roeselová, M.; Sodeau, J.R. *Atmos. Chem. Phys. Discuss.* **2014,** *14*, 1.

[9] Hodgson, A.; Haq, S. *Surf. Sci. Rep.* **2009**, *64*, 381.

[10] Carrasco, J.; Michaelides, A.; Forster, M.; Raval, R.; Hodgson, A. *Nature Mat.* **2009**, *8*, 427.

[11] Thiel, P.A.; Madey, T.E. *Surf. Sci. Rep.* **1987**, *7*, 211.

[12] Maier, S.; Salmeron, M. *Acc. Chem. Res.* **2015**, *48*, 2783.

[13] Feibelman, P.J. *Science* **2002**, *295*, 99.

[14] Shavorskiy, A.; Gladys, M. J.; Held, G. *Phys. Chem. Chem. Phys.* **2008**, *10*, 6150.

[15] Clay, C.; Haq, S.; Hodgson, A. *Phys. Rev. Lett.* **2004**, *92*, 046102.

[16] Forster, M.; Raval, R.; Hodgson, A.; Carrasco, J.; Michaelides, A. *Phys. Rev. Lett.* **2011**, *106*, 046103.

[17] Okuyama, H.; Hamada, I. *Journal of Physics D-Applied Physics* **2011**, *44*, 464004.

[18] Michaelides, A.; Ranea, V.A.; de Andres, P.L.; King, D. A. *Phys. Rev. Lett.* **2003**, *90*, 216102.

[19] Salmeron, M.; Bluhm, H.; Tatarkhanov, N.; Ketteler, G.; Shimizu, T. K.; Mugarza, A.; Deng, X. Y.; Herranz, T.; Yamamoto, S.; Nilsson, A. *Faraday Disc.* **2009**, *141*, 221.

[20] Cerda, J.; Michaelides, A.; Bocquet, M. L.; Feibelman, P. J.; Mitsui, T.; Rose, M.; Fomin, E.; Salmeron, M. *Phys. Rev. Lett.* **2004**, *93*, 116101.

[21] Maier, S.; Stass, I.; Cerda, J.I.; Salmeron, M. *Phys. Rev. Lett.* **2014**, *112*, 126101.

[22] Standop, S.; Redinger, A.; Morgenstern, M.; Michely, T.; Busse, C. *Phys. Rev. B* **2010**, *82*, 161412.

[23] Thürmer, K.; Bartelt, N. C. *Phys. Rev. Lett.* **2008**, *100*, 186101.

[24] Kumagai, T.; Kaizu, M.; Hatta, S.; Okuyama, H.; Aruga, T.; Hamada, I.; Morikawa, Y. *Phys. Rev. Lett.* **2008**, *100*, 166101.

[25] Kumagai, T.; Okuyama, H.; Hatta, S.; Aruga, T.; Hamada, I. *J. Chem. Phys.* **2011**, *134*, 024703.

[26] Motobayashi, K.; Matsumoto, C.; Kim, Y.; Kawai, M. *Surf. Sci.* **2008**, *602*, 3136.

[27] Ranea, V.A.; Michaelides, A.; Ramirez, R.; Verges, J.A.; de Andres, P.L.; King, D.A. *Phys. Rev. Lett.* **2004**, *92*, 136104.

[28] Michaelides, A.; Morgenstern, K. *Nature Mat.* **2007**, *6*, 597.

[29] Haq, S.; Clay, C.; Darling, G. R.; Zimbitas, G.; Hodgson, A. *Phys. Rev. B* **2006**, *73*, 115414

[30] Nie, S.; Feibelman, P. J.; Bartelt, N. C.; Thurmer, K. *Phys. Rev. Lett.* **2010**, *105*, 026102.

[31] Ogasawara, H.; Brena, B.; Nordlund, D.; Nyberg, M.; Pelmenschikov, A.; Pettersson, L. G. M.; Nilsson, A. *Phys. Rev. Lett.* **2002**, *89*, 276102.

[32] Haq, S.; Harnett, J.; Hodgson, A. *Surf. Sci.* **2002**, *505*, 171.

[33] Maier, S.; Stass, I.; Mitsui, T.; Feibelman, P. J.; Thurmer, K.; Salmeron, M. *Phys. Rev. B* **2012**, *85*, 155434.

[34] McBride, F.; Darling, G. R.; Pussi, K.; Hodgson, A. *Phys. Rev. Lett.* **2011**, *106*, 226101.

[35] Massey, A.; McBride, F.; Darling, G. R.; Nakamura, M.; Hodgson, A. *Phys. Chem. Chem. Phys.* **2014**, *16*, 24018.

[36] Cox, S. J.; Kathmann, S. M.; Purton, J. A.; Gillan, M. J.; Michaelides, A. *Phys. Chem. Chem. Phys.* **2012**, *14*, 7944.

[37] Zhu, C.Q.; Li, H.; Huang, Y.F.; Zeng, X.C.; Meng, S. *Phys. Rev. Lett.* **2013**, *110*, 126101.

[38] Michaelides, A.; Hu, P. *J. Chem. Phys.* **2001**, *114*, 513.

[39] Michaelides, A.; Hu, P. *J. Am. Chem. Soc.* **2001**, *123*, 4235.

[40] Kumagai, T.; Shiotari, A.; Okuyama, H.; Hatta, S.; Aruga, T.; Hamada, I.; Frederiksen, T.; Ueba, H. *Nature Mat.* **2012**, *11*, 167.

[41] Forster, M.; Raval, R.; Carrasco, J.; Michaelides, A.; Hodgson, A. *Chem. Sci.* **2012**, *3*, 93.

[42] Mehlhorn, M.; Morgenstern, K. *New Journal of Physics* **2009**, *11*, 093015.

[43] Haq, S.; Hodgson, A. *J. Phys. Chem. C* **2007**, *111*, 5946.

[44] Zimbitas, G.; Gallagher, M. E.; Darling, G. R.; Hodgson, A. *J. Chem. Phys.* **2008**, *128*, 074701.

[45] Kimmel, G. A.; Petrik, N. G.; Dohnálek, Z.; Kay, B. D. *Phys. Rev. Lett.* **2005**, *95*, 166102.

[46] Zimbitas, G.; Haq, S.; Hodgson, A. *J. Chem. Phys.* **2005**, *123*, 174701.

[47] Thürmer, K.; Bartelt, N. C. *Phys. Rev. B* **2008**, *77*, 195425.

[48] Schiros, T.; Haq, S.; Ogasawara, H.; Takahashi, O.; Öström, H.; Andersson, K.; Pettersson, L. G. M.; Hodgson, A.; Nilsson, A. *Chem. Phys. Lett.* **2006**, *429*, 415.

[49] Khaliullin, R.Z.; Kühne, T.D. *Phys. Chem. Chem. Phys.* **2013**, *15*, 15746.

[50] Carrasco, J; Santra, B; Klimeš, J.; Michaelides, A. *Phys. Chem. Chem. Phys.* **2010**, *12*, 6375.

[51] Carrasco, J; Santra, B.; Klimeš, J.; Michaelides, A. *Phys. Rev. Lett.* **2011**, *106*, 026101.

[52] Ma, J.; Michaelides. A.; Alf`e, D.; Schimka, L.; Kresse, G., Wang E. *Phys. Rev. B* **2011**, *84*, 003402.

[53] Becke, A.D. *J. Chem. Phys.* **2014**, *140*, 301.

[54] Taylor, C. D.; Neurock, M. *Current Opinion in Solid State and Materials Science* **2005**, *9*, 49.

[55] Norskov, J.K.; Bligaard, T.; Rossmeisl, J.; Christensen, C.H. *Nature Chemistry* **2009**, *1*, 37.

[56] Somorjai, G.A.; Li, Y. *Introduction to Surface Chemistry and Catalysis* (Wiley, 2 ed., Hoboken, NJ, **2010**).

[57] Aurbach, D. *Journal of Power Sources* **2000**, *89*, 206.

[58] Vayenas, C.G. *Modern Aspects of Electrochemistry* Vol. 36 (Wiley, 2ed., **2002**).

[59] Bard, A.; Faulkner, L. *Electrochemical methods fundamentals and application*, Vol. 1; Wiley & Sons," New York , 339, **2001**.

[60] Verdaguer, A; Sacha, G.M.; Bluhm, H.; Salmeron, M. *Chem. Rev.* , **2006**, *106*, 1478.

[61] Henderson, M. A. *Surface Science Reports* **2002**, *46*, 1.

[62] Schiros, T.; Takahashi, O.; Andersson, K. J.; Öström, H.; Pettersson, L. G.; Nilsson, A.; Ogasawara, H. *The Journal of Chemical Physics* **2010**, *132*, 094701.

[63] Kimmel, G.A.; Petrik, N.G.; Dohnalek, Z.; Kay, B.D. *Phys. Rev. Lett.* **2005**, *95*, 166102.

[64] Yamamoto, S.; Andersson, K.; Bluhm, H.; Ketteler, G.; Starr, D.E.; Schiros, Th.; Ogasawara, H.; Pettersson, L.G.M.; Salmeron, M.; Nilsson, A. *J. Phys. Chem. C* **2007**, *111*, 7848.

[65] Andersson, K.; Ketteler, G.; Bluhm, H.; Yamamoto, S.; Ogasawara, H.; Pettersson, L.G.M.; Salmeron, M.; Nilsson, A. *J. Am. Chem. Soc.* **2008**, *130*, 2793.

[66] Hansen, H.A.; Viswanathan, V.; Norskov, J.K. J. Phys. Chem. J.K. **2014**, *118*, 6706.

[67] Bovensiepen, U.; Gahl, C.; Stahler, J.; Bockstedte, M..; Meyer, M.; Baletto, F.; Scandolo, S.; Zhu, X.-Y.; Rubio, A.; Wolf, M. *J. Phys. Chem. C* **2008**, *113*, 979.

[68] Velasco-Velez, J.-J.; Wu, C-H.; Pascal, T.A.; Wan, L.W.; Guo, J.; Prendergast. D.; Salmeron, M. *Science*, **2014**, *346*, 831.

[69] Limmer, D.T.; Willard, A.P.; Madden, P.; Chandler, D. *PNAS* **2013**, *110*, 4200.

[70] Kimmel, G. A.; Petrik, N. G.; Dohnálek, Z.; Kay, B. D. *Phys. Rev. Lett.* **2005**, *95*, 166102.

[71] Hamada, I.; Lee, K.; Morikawa, Y. *Phys. Rev. B* **2010**, *81*, 115452.

[72] Carrasco, J. Klimeš, J.; Michaelides, A. *J. Chem. Phys.* **2013**, *138*, 024708.

[73] Meng, S.; Wang, E. G.; Gao, S.W. *Phys. Rev. B* **2004**, *69*, 195404.

[74] Poissier, A.; Ganeshan, S.; Fernández-Serra, M.V. Phys. Chem. Chem. Phys. **2011**, *13*, 3375.

[75] Safran, S. *Statistical Thermodynamics of Surfaces and Interfaces*; Addison-Wesley, New York, **1994**; Vol. 103.

[76] Tonigold, K.; Groß, A. *Journal of Computational Chemistry* **2012**, *33*, 695.

[77] VandeVondele, J.; Borštnik, U.; Hutter, J. *Journal of Chemical Theory and Computation* **2012**, *8*, 3565.

[78] Meng, S.; Wang, E.G.; Gao, S. *Phys. Rev. B* **2004**, *69*, 195404.

[79] Perdew, J.P.; Burke, K.; Ernzerhof, M. *Phys. Rev. Lett.* **1996**, 77, 3865.

[80] Hammer, B.; Hansen, L.B.; Nørskov, J.K. *Phys. Rev. B* **1999**, *59*, 7413.

[81] Tatarkhanov, M.; Ogletree, D.F.; Rose, F.; Mitsui, T.; Fomin, E.; Maier, S.; Rose, M.; Cerdá, J.I.; Salmeron, M. *J. Am. Chem. Soc.* **2009**, *131*, 18425.

[82] Feibelman, P.J.; Kimmel, G.A.; Smith, R.S.; Petrik, N.G.; Zubkov, T.; Kay, B.D. *J. Chem. Phys.* **2011**, *134*, 204702.

[83] Klimes, J.; Michaelides, A. *J. Chem. Phys.* **2012**, *137*, 120901.

[84] Tkatchenko, A. *Adv. Funct. Mat.* **2015**, *25*, 2054.

[85] Schnur, S.; Groß, A. *New Journal of Physics* **2009**, *11*, 125003.

[86] Møgelhøj, A.; Kelkkanen, A.K.; Wikfeldt, K.T.; Schiøtz, J.; Mortensen, J.J.; Pettersson, L.G.M.; Lundqvist, B.I.; Jacobsen, K.W.; Nilsson, A.; Nørskov, J.K. *J. Phys. Chem. B* **2011**, *115*, 14149.

[87] Carrasco, J. ; Santra, B. ; Klimeš, J.; Michaelides, A. *Phys. Rev. Lett.* **2011**, *106*, 026101.

[88] Skúlason, E.; Tripkovic, V.; Bjo□rketun, M.E.; Gudmundsdóttir, S.; Karlberg, G.; Rossmeisl, J.; Bligaard, T.; Jónsson, H.; Nørskov, J. K. *J. Phys. Chem. C* **2010**, *114*, 18182.

[89] Rossmeisl, J.; Chan, K.; Ahmed, R.; Tripković, V.; Björketun, M;. Arten, E. *Phys. Chem. Chem. Phys.* **2013**, *15*, 10321.

[90] Pedroza, L.; Poisier, A.; Fernández-Serra, M.V.; *J. Chem. Phys*., **2015**, *142*, 034706.

[91] Tonigold, K.; Groß, A. *J. Comp. Chem.* **2012**, *33*, 695.

[92] Filhol, J.-S.; Neurock, M. *Ang. Chem. Int. Ed.* **2006**, *118*, 416.

[93] Chen, H.; Gan, W.; Lu, R.; Guo, Y.; Wang, H.-F. *J. Phys. Chem. B*, **2005**, *109*, 8064.

[94] Roman, T.; Groß, A. *Cat. Today* **2013**, *202*, 183.

[95] Lynch, G.C.; Pettitt, B.M. *J. Chem. Phys.* **1997**, *107*, 8594.

[96] Nielsen, M.; Björketun, M.E.; Hansen, M.H.; Rossmeisl, J. *Surf. Sci.*, **2015**, *631*, 2.

[97] Cheng, J.; Sprik, M. *Phys. Chem. Chem. Phys.* **2012**, *14*, 11245.

[98] Koper, M.T. In *Modern Aspects of Electrochemistry, Vol. 36*; Springer, **2003**; 51–130.

[99] Skúlason, E.; Karlberg, G.S.; Rossmeisl, J.; Bligaard, T; Greeley, J.; Jónsson, H; Norskov, J.K. *Phys. Chem. Chem. Phys.* **2007**, *9*, 3241.

[100] Lozovoi, A.Y.; Alavi, A.; Kohanoff, J.; Lynden-Bell, R M. *J. Chem. Phys.* **2001**, *115*, 1661.

[101] Bonnet, N.; Morishita, T.; Sugino, O.; Otani, M. *Phys. Rev. Lett.* **2012**, *109*, 266101.

[102] Crispin, X.; Geskin, V.; Bureau, C.; Lazzaroni, R.; Schmickler, W.; Bredas, J. *J. Chem. Phys.* **2001**, *115*, 10493.

[103] Hamada, I.; Sugino, O.; Bonnet, N.; Otani, M.; *Phys. Rev. B* **2013**, *88*, 155427.

[104] Jinnouchi, R.; Anderson, A. B. *Phys. Rev. B* **2008**, *77*, 245417.

[105] Taylor, C.; Kelly, R.G.; Neurock, M. *J. Electrochem. Soc.* **2007**, *154*, F55.

[106] Bonnet, N.; Marzari, N. *Phys. Rev. Lett.* **2013**, *110*, 086104.

[107] Spohr, E.; Heinzinger, K. *Chem. Phys. Lett.* **1986**, *123*, 218.

[108] Spohr, E.; Heinzinger, K. *Electrochimi. Acta* **1988**, *33*, 1211.

[109] Siepmann, J.I.; Sprik, M. *J. Chem. Phys.* **1995**, *102*, 511.

[110] Golze, D.; Iannuzzi, M.; Nguyen, M.-T.; Passerone, D.; Hutter, J. *J. Chem. Theory Comp.* **2013**, *9*, 5086.

[111] Wilhelm, F.; Schmickler, W.; Nazmutdinov, R.R.; Spohr, E. *J. Phys. Chem. C* **2008**, *112*, 10814.

[112] Schmickler, W.; Wilhelm, F.; Spohr, E. *Electrochimica Acta* **2013**, *101*, 341.

[113] Wilhelm, F.; Schmickler, W.; Spohr, E. *J. Phys.: Cond. Matt.* **2010**, *822*, 175001.

[114] Cao, Z.; Kumar, R., Peng, Y.; Voth, G.A. *J. Phys. Chem. B* **2014**, *118*, 845.

[115] Spohr, E. *Chem. Phys.* **1990**, *141*, 87.

[116] Willard, A.P.; Limmer, D.T.; Madden, P. A.; Chandler, D. *J. Chem. Phys.* **2013**, *138*, 184702.

[117] Cao, Z.; Kumar, R.; Peng, Y.; Voth, G. A. *J. Phys. Chem. B* **2014**, *118*, 8090.

[118] Glosli, J.N.; Philpott, M.R. *J. Chem. Phys* **1992**, *96*, 6962.

[119] Rose, D.A.; Benjamin, I. *J. Chem. Phys.* **1993**, *98*, 2283.

[120] Spohr, E. *J. Mol. Liq.* **1995**, *64*, 91.

[121] Spohr, E. *Chem. Phys. Lett.* **1993**, *207*, 214.

[122] Limmer, D.T.; Willard, A.P.; Madden, P.A.; Chandler, D. *J. Phys. Chem. C* **2015**, *119*, 24016.

[123] Limmer, D.T.; Willard, A.P. *Chem. Phys. Lett.* **2015**, *620*, 144.

[124] Limmer, D.T.; Merlet, C.; Salanne, M.; Chandler, D.; Madden, P.A.; Van Roij, R.; Rotenberg, B. *Phys. Rev. Lett.* **2013**, *111*, 106102.

[125] Bonthuis, D. J. ; Gekle, S.; Netz, R.R. *Phys. Rev. Lett.* **2011**, *107*, 166102.

[126] Reed, S.K.; Madden, P.A.; Papadopoulos, A. *J. Chem. Phys.* **2008**, *128*, 124701.

[127] Heinzinger, K.; Spohr, E. *Electrochim. Acta* **1989**, *34*, 1849.

[128] Willard, A.P.; Reed, S.K.; Madden, P.A.; Chandler, D. *Faraday Disc.* **2009**, *141*, 423.

[129] Knight, C.; Voth, G.A. *Acc. Chem. Res.* **2011**, *45*, 101.

[130] Lorenz, S.; Scheffler, M.; Gross, A. *Phys. Rev. B* **2006**, *73*, 115431.

[131] Bartok, A.P.; Csanyi, G *Int. J. Quantum Chem.*, **2015**, *115*, 1051.

[132] Babin, V.; Medders, G.R.; Paesani, F. *J. Phys. Chem. Lett.* **2012**, *3*, 3765.

[133] Sposito, G. *The Surface Chemistry of Soils*, Oxford University Press, **1984**.

[134] Hochella, M. F.; White, A.F. *Reviews in Mineralogy and Geochemistry* **1990**, *23,* 1.

[135] Parks, G.A. *Reviews in Mineralogy and Geochemistry* **1990**, *23,* 133.

[136] Du, Q.; Superfine, R.; Freysz, E.; Shen, Y. R. *Phys. Rev. Lett.* **1994**, *72,* 238.

[137] Hu, J.; Xiao, X.D.; Ogletree, D. F.; Salmeron, M. *Science* **1995**, *268*, 267.

[138] Bluhm, H. *J. Electron Spectrosc. Relat. Phenom.* **2010**, *177*, 71.

[139] Fenter, P.; Sturchio, N.C. *Prog. Surf. Sci.* **2004**, *77*, 171.

[140] Teschke, O.; Ceotto, G.; de Souza, E.F.; *Chem. Phys. Lett.* **2000**, *326,* 328.

[141] Henderson, M.A. *Surf. Sci. Rep.* **2011**, *66*, 185.

[142] Brown, Jr., G.E.; Calas G. *Geochem. Persp.* **2012**, *1*, 483.

[143] Odelius, M.; Bernasconi, M; Parrinello, M. *Phys. Rev. Lett.* **1997**, *78*, 2855.

[144] Miranda, P.B.; Xu, L.; Shen, Y.R.; Salmeron, M. *Phys. Re*v. *Lett.* **1998**, *81*, 5876.

[145] Bluhm, H.; Inoue, T.; Salmeron, M. *Surf. Sci.* **2000**, *462*, L599.

[146] Kaya, S.; Schlesinger, D.; Yamamoto, S.; Newberg, J.T.; Bluhm, H.; Ogasawara, H.; Kendelewicz, T.; Brown, Jr., G.E.; Pettersson, L.G.M.; Nilsson, A. *Sci. Rep.* **2013**, *3*, 1074.

[147] G.E. Ewing *Chem. Rev.* 2006, **106**, 1511.

[148] Cheng, L.; Fenter, P.; Nagy, K.L.; Schlegel, M.L.; Sturchio, N.C. *Phys. Rev. Lett.* **2001**, *87*, 156103.

[149] Park, S.-H.; Sposito, G. *Phys. Rev. Lett.* **2002**, *89*, 085501.

[150] Leng Y.; Cummings, P.T. *Phys. Rev. Lett.* **2005**, *94*, 026101.

[151] Ostroverkhov, V.; Waychunas, G.A.; Shen, Y.R. *Phys. Rev. Lett.* **2005**, *94*, 046102.

[152] Leung, K; Nielsen, I.M.B.; Criscenti. L.J. *J. Am. Chem. Soc.* **2009**, *131*, 18358.

[153] Gupta, P.K.; Meuwly, M. *Faraday Discuss.* **2013**, *167*, 329.

[154] Siegbahn, H. *J. Phys. Chem.* **1985**, *89*, 897.

[155] Salmeron, M.; Schlögl, R. *Surf. Sci. Rep.* **2008**, *63*, 169.

[156] Starr, D.E.; Liu, Z.; Hävecker, M.; Knop-Gericke, A.; Bluhm, H. *Chem. Soc. Rev.* **2013**, *42*, 5833.

[157] Ketteler, G.; Yamamoto, S.; Bluhm, H.; Andersson, K.; Starr, D.E.; Ogletree, D.F.; Ogasawara, H.; Nilsson, A.; Salmeron, M. *J. Phys. Chem. C* **2007**, *111*, 8278.

[158] Yamamoto, S.; Kendelewicz, T.; Newberg, J.T.; Ketteler, G.; Starr, D.E.; Mysak, E.R.; Andersson, K.; Ogasawara, H.; Bluhm, H.; Salmeron, M.; Brown, Jr., G.E.; Nilsson, A. *J. Phys. Chem. C* **2010**, *114*, 2256.

[159] Kendelewicz, T.; Kaya, S.; Newberg, J.T.; Bluhm, H.; Mulakaluri, N.; Moritz, W.; Scheffler, M.; Nilsson, A.; Pentcheva, R.; Brown, Jr., G. E. *J. Phys. Chem. C* **2013**, *117*, 2719.

[160] Newberg, J.T.; Starr, D.E.; Porsgaard, S.; Yamamoto, S.; Kaya, S.; Mysak, E.R.; Kendelewicz, T.; Salmeron, M.; Brown, Jr., G.E.; Nilsson, A.; Bluhm, H. *Surf. Sci.* **2011**, *605*, 89.

[161] Newberg, J.T.; Starr, D.E.; Porsgaard, S.; Yamamoto, S.; Kaya, S.; Mysak, E.R.; Kendelewicz, T.; Salmeron, M.; Brown, Jr., G.E.; Nilsson, A.; Bluhm, H. *J. Phys. Chem. C* **2011**, *115*, 12864.

[162] Verdaguer, A.; Weis, Ch.D.; Oncins, G.; Ketteler, G.; Bluhm, H.; Salmeron, M. *Langmuir* **2007**, *23*, 9699.

[163] Deng, X.; Herranz, T.; Weis, Ch.; Bluhm, H.; Salmeron, M. *J. Phys. Chem. C* **2008**, *112*, 9668.

[164] Shavorskiy, A.; Müller, K.; Newberg, J.T.; Starr, D.E.; Bluhm, H. *J. Phys. Chem. C* **2014**, *118*, 29340.

[165] Deng, X.; Verdaguer, A.; Herranz, T.; Weiss, Ch.D.; Bluhm, H.; Salmeron, M. *Langmuir* **2008**, *24* 9474.

[166] Włodarczyk, R.; Sierka, M.; Kwapień, K.; Sauer, J.; Carrasco, E.; Aumer, A.; Gomes, J.F.; Sterrer, M.; Freund, H.-J. *J. Phys. Chem. C*, **2011**, *115*, 6764.

[167] Hu, X.L.; Klimes, J.; Michaelides, A. *Phys. Chem. Chem. Phys.* **2010**, *12*, 3953.

[168] Foster, M.; D'Agostina, M.; Passno, D. *Surf. Sci.* **2005**, *590*, 31.

[169] Diebold, U. *Surf. Sci. Rep.* **2003**, *48*, 53.

[170] Teobaldi, G.; Hofer, W.A.; Bikondoa, O.; Pang, C.L.; Cabailh, G.; Thornton, G. *Chem. Phys. Lett.* **2007**, *437*, 73.

[171] Liu, L.-M.; Zhang, C.; Thornton, G.; Michaelides, A. *Phys. Rev. B* **2010**, *82*, 161415.

[172] Langel, W. *Surf. Sci.* **2002**, *496*, 141.

[173] Kowalski, P.M.; Meyer, B.; Marx, D. *Phys. Rev. B* **2009**, *79* ,115410.

[174] Lindan, P.J.D.; Harrison, N.M.; Holender, J.M.; Gillan, M.J. *Chem. Phys. Lett.* **1996**, *261*, 246.

[175] Liu, L.M.; Zhang, C.; Thornton, G.; Michaelides, A. *Phys. Rev. B* **2012,** *85*, 167402.

[176] Cheng, J.; Sprik, M. *J. Chem. Theory Comput.* **2010**, *6*, 880.

[177] Cheng, J.; Sprik, M. *Phys. Rev. B* **2010**, *82*, 081406.

[178] Serrano, G.; Bonanni, B.; Di Giovannantonio, M.; Kosmala, T.; Schmid, M.; Diebold, U.; Di Carlo, A.; Cheng, J.; VandeVondele, J.; Wandelt, K.; Goletti, C. *Adv. Mat. Interfaces* **2015**, *2*, 1500246.

[179] Bredow, Th.; Giordano, L.; Cinquini, F.; Pacchioni G. *Phys. Rev. B* **2004**, *70*, 035419.

[180] Liu, L.-M.; Zhang, C.; Thornton, G.; Michaelides, A. *Phys. Rev. B* **2010**, *82*, 161415.

[181] Liu, L.-M.; Zhang, C.; Thornton, G.; Michaelides, A. *Phys. Rev. B* **2012**, *85*, 167402.

[182] Petrik, N.G.; Kimmel, G.A. *Phys. Rev. Lett.* **2007**, *99*, 196103.

[183] Nemšák, S.; Shavorskiy,A.; Karslioglu, O.; Zegkinoglou, I.; Greene, P.K.; Burks, E.C.; Liu, K.; Rattanachata, A.; Conlon, C.S.; Keqi, A.; Salmassi, F.; Gullikson, E.M.; Yang, S.-H.; Bluhm, H.; Fadley, C.S. *Nat. Comm.* **2014**, *5*, 5441.

[184] Fadley, C.S. *J. Electron Spectrosc. Relat. Phenom.* **2013**, *190*, 165.

[185] Trainor, T.P.; Chaka, A.M.; Eng, P.J.; Newville, M.; Waychunas, G.A.; Catalano, J.G.; Brown Jr., G.E. *Surf. Sci.* **2004**, *573*, 204.

[186] Catalano, J.G. *Geochimica et Cosmochimica Acta* **2011**, *75*, 2062.

[187] Kerisit, S. *Geochimica et Cosmochimica Acta* **2011**, *75*, 2043.

[188] Liu, H.; Chen, T.; Frost, R.L. *Chemosphere* **2014**, *103*, 1.

[189] Gaigeot, M.P.; Sprik, M.; Sulpizi, M. *J. Phys.: Condens. Matter* **2012**, *24*, 124106.

[190] Huang, P.; Pham, T.A.; Galli, G.; Schwegler, E. *J. Phys. Chem. C* **2014**, *118*, 8944.

[191] Argyris, D.; Ho, T.A.; Cole, D.R.; Striolo, A. *J. Phys. Chem. C* **2011**, *115*, 2038.

[192] Janeček, J.; Netz, R.R.; Flörsheimer, M.; Klenze, R.; Schimmelpfennig, B.; Polly, R. *Langmuir* **2014**, *30*, 2722.

[193] Israelachvili, J.N., *Intermolecular and Surface Forces* 3rd Ed.; Elsevier: Oxford, **2011**; p 674.

[194] Chandler, D. *Nature* **2005**, *437*, 640.

[195] Richmond, G.L. *Chem. Rev.* **2002,** *102*, 2693.

[196] Du, Q.; Freysz, E.; Shen, Y.R. *Science* **1994,** *264*, 826.

[197] Hopkins, A.J.; McFearin, C.L.; Richmond, G.L. *J. Phys. Chem. C* **2011**, *115*, 11192.

[198] Scatena, L.F.; Brown, M.G.; Richmond, G.L. *Science* **2001,** *292*, 908.

[199] Ye, S.; Nihonyanagi, S.; Uosaki, K. *Phys. Chem. Chem. Phys.* **2001,** *3*, 3463.

[200] Tyrode, E.; Liljeblad, J.F D. *J. Phys. Chem. C* **2013,** *117*, 1780.

[201] Donaldson, S.H.; Røyne, A.; Kristiansen, K.; Rapp, M.V.; Das, S.; Gebbie, M.A.; Lee, D.W.; Stock, P.; Valtiner, M.; Israelachvili, J. *Langmuir* **2014**, *31*, 2051.

[202] Hammer, M. U.; Anderson, T. H.; Chaimovich, A.; Shell, M. S.; Israelachvili, J. *Faraday Discuss.* **2010,** 146, 299.

[203] Li, Z.; Yoon, R.-H. *J. Colloid Interface Sci.* **2013**, *392*, 369.

[204] Wang, J.; Yoon, R.-H.; Eriksson, J. C. *J. Colloid Interface Sci.* **2011**, *364*, 257.

[205] Eriksson, J.C.; Ljunggren, S.; Claesson, P.M. *J. Chem. Soc. Faraday Trans.* **1989,** *85*, 163.

[206] Jensen, T.R.; Østergaard Jensen, M.; Reitzel, N.; Balashev, K.; Peters, G.H.; Kjaer, K.; Bjørnholm, T., *Phys. Rev. Lett.* **2003,** *90*, 086101.

[207] Mezger, M.; Sedlmeier, F.; Horinek, D.; Reichert, H.; Pontoni, D.; Dosch, H. *J. Am. Chem. Soc.* **2010,** *132*, 6735.

[208] Poynor, A.; Hong, L.; Robinson, I.K.; Granick, S.; Zhang, Z.; Fenter, P. A. *Phys. Rev. Lett.* **2006,** *97*, 266101.

[209] Uysal, A.; Chu, M.; Stripe, B.; Timalsina, A.; Chattopadhyay, S.; Schlepütz, C.; Marks, T.; Dutta, P. *Phys. Rev. B* **2013,** *88*, 035431.

[210] Doshi, D.A.; Watkins, E.B.; Israelachvili, J.N.; Majewski, J. *Proc. Natl. Acad. Sci. U. S. A.* **2005,** *102*, 9458.

[211] Maccarini, M.; Steitz, R.; Himmelhaus, M.; Fick, J.; Tatur, S.; Wolff, M.; Grunze, M.; Janec□ek, J.; Netz, R.R. *Langmuir* **2006,** *23*, 598.

[212] Mezger, M.; Reichert, H.; Schöder, S.; Okasinski, J.; Schröder, H.; Dosch, H.; Palms, D.; Ralston, J.; Honkimäki, V. *Proc. Natl. Acad. Sci.* **2006,** *103*, 18401.

[213] Chattopadhyay, S.; Uysal, A.; Stripe, B.; Ha, Y.-g.; Marks, T.; Karapetrova, E.; Dutta, P. *Phys. Rev. Lett.* **2010,** *105*, 037803.

[214] Hopkins, A.J.; McFearin, C. L.; Richmond, G.L. *J. Phys. Chem. C* **2011**, *115*, 11192.

[215] Brzoska, J.B.; Azouz, I.B.; Rondelez, F. *Langmuir* **1994**, *10*, 4367.

[216] Knock, M.M.; Bell, G.R.; Hill, E.K.; Turner, H.J.; Bain, C.D. *J. Phys. Chem. B* **2003,** *107*, 10801.

[217] Strazdaite, S.; Versluis, J.; Backus, E.H.G.; Bakker, H.J. *J. Chem. Phys.* **2014**, *140*, 4711.

[218] Day, J.P.R.; Bain, C.D. *Phys. Rev. E* **2007,** *76*, 041601.

[219] Samson, J.-S.; Scheu, R.; Smolentsev, N.; Rick, S. W.; Roke, S. *Chem. Phys. Lett.* **2014,** 615, 124.

[220] Agmon, N.; Bakker, H.J.; Campen, R.K.; Henchman, R.H.; Pohl, P.; Roke, S.; Thämer, M.; Hassanali, A. *Chem. Rev.* **2016**, this issue.

[221] Intergovernmental Panel on Climate Change. *Climate Change 2013: The Physical Basis*. (**2013**).

[222] Johnson, C.M.; Baldelli, S. *Chem. Rev.* **2014**, *114*, 8416.

[223] Richmond, G.L. *Annu. Rev. Phys. Chem.* **2001**, *52*, 357.

[224] Petersen, P.B.; Saykally, R.J. *Chem. Phys. Lett.* **2008**, *458*, 255.

[225] Winter, B. *Nuclear Instrum. Meth. A* **2009**, *601*, 139.

[226] Als-Nielson, J. ; Jacquemain, D.; Kjaer, K.; Leveiller, F.; Lahav, M.; Leiserowitz, L. *Phys. Rep*. **1994**, *246*, 251.

[227] Stefaniu, C.; Brezesinski, G. *Current Opinion in Colloid & Interface Science* **2014**, *19*, 216.

[228] Hub, J.S.; Wolf, M.G.; Caleman, C.; v. Maaren, P.J.; Groenhof, G..; v. d. Spoel, D. *Chem. Sci.* **2014**, *5*, 1745.

[229] Sun, L.; Li, X.; Hede, T.; Tu, Y.; Leck, C.; Ågren, H. *J. Phys. Chem. B* **2012**, *116*, 3198.

[230] Jungwirth, P.; Winter, B. *Annu. Rev. Phys. Chem.* **2008**, *59*, 343.

[231] Sovago, M.; Campen, R.K.; Wurpel, G.W.; Muller, M.; Bakker, H.J.; Bonn, M. *Phys. Rev. Lett.* **2008**, *100*, 173901.

[232] Mishra, H.; Enami, S.; Nielsen, R.J.; Stewart, L.A.; Hoffmann, M.R.; Goddard III, W.A.; Colussi, A.J. *PNAS* **2012**, *109*, 18679.

[233] Onsager, L.; Samaras, N.N.T. *J. Chem. Phys.* **1934**, *2*, 528.

[234] Otten, D.E.; Shaffer, P.R.; Geissler, P.L.; Saykally, R.J. *PNAS* **2012**, *109*, 701.

[235] Caleman, C. *PNAS* **2011**, *108*, 6838.

[236] Huang, Z.; Hua, W.; Verreault, D.; Allen, H.C. *J. Phys. Chem. A* **2013**, *117*, 6346.

[237] Piatkowski. L.; Zhang, Z.; Backus, E.H.G.; Bakker, H.J.; Bonn, M. *Nature Comm.* **2014**, *5*, 4083.

[238] Ottosson, N.; Heyda, J.; Wernersson, E.; Pokapanich, W.; Svensson, S.; Winter, B.; Öhrwall, G.; Jungwirth, P.; Björneholm, O. *Phys. Chem. Chem. Phys.* **2010**, *12*, 10693.

[239] Venkateshwaran V.; Vembanur S.; Garde S. *PNAS* **2014**, *111*, 8729.

[240] Werner J.; Wernersson E.; Ekholm V.; Ottosson N.; Ohrwall G.; Heyda J.; Persson I.; Söderström J.; Jungwirth P.; Björneholm O. *J. Phys. Chem. B.* **2014**, *118*, 7119.

[241] Xu, M.; Tang, C.Y.; Jubb, A.M.; Chen, X.; Allen, H.C. *J. Phys. Chem. C* **2009**, *113*, 2082.

[242] Plath, K.L.; Valley, N.A.; Richmond, G.L. *J. Phys. Chem.* A **2013**, *117*, 11514.

[243] Okur, H.I.; Kherb, J.; Cremer, P.S. *J. Am. Chem. Soc.* **2013**, *135*, 5062.

[244] Donaldson, D.J., Vaida, V. *Chem. Rev.* **2006**, *106*, 1445.

[245] Can, S.Z.;. Mago, D.D.; Esenturk, O.; Walker, R.A. *J. Phys. Chem. C* **2007**, *111*, 8739.

[246] Walz, M.-M., Caleman, C., Werner, J., Ekholm, V., Lundberg, D., Prisle, N.L., Öhrwall, G., Björneholm, O. *Phys. Chem. Chem. Phys.* **2015,** *17*, 14036.

[247] Johnson, C.M.; Tyrode, E.; Kumpulainen, A.; Leygraf, C. *J. Phys. Chem. C* **2009**, *113*, 13209.

[248] Tyrode, E.; Johnson, C.M.; Baldelli, S.; Leygraf, C.; Rutland, M.W. *J. Phys. Chem. B* **2005**, *109*, 329.

[249] Chen, H.; Gan, W.; Wu, B.-H.; Wu, D.; Guo, Y.; Wang, H.-F. *J. Phys. Chem. B* **2005**, *109*, 8053.

[250] Chen, H.; Gan, W.; Lu, R.; Guo, Y.; Wang, H.-F. *J. Phys. Chem. B* **2005**, *109*, 8064.

[251] Kunz, W.; Henle, J.; Ninham, B.W. *Curr. Opin. Colloid Interface Sci.* **2004**, *9*, 19.

[252] Wang, C.; Lei, Y.D.; Endo, S.; Wania, F. *Environ. Sci. Technol.* **2014**, *48*, 13238.

[253] H. I. Okur, J. Kherb, P. S. Cremer, JACS 135 (2013) 5062-5067

[254] Pruyne, J.G.; Lee, M.T.; Fábri, C.; Redondo, A.B.; Kleibert, A.; Ammann, M.; Brown, M.A.; Krisch, M.J. *J. Phys. Chem. C*, in press.

[255] Ottosson, N.; Wernersson, E.; Söderström, J.; Pokapanich, W.; Kaufmann, S.; Svensson, S.; Persson, I.; Öhrwall, G.; Björneholm, O. *Phys. Chem. Chem. Phys.* **2011**, *13*, 12261.

[256] Lewis, T.; Winter, B.; Stern, A.C.; Baer, M.D.; Mundy, C.J.; Tobias, D.J.; Hemminger, J.C. *J. Phys. Chem. C* **2011**, *115*, 21183.

[257] Adriaanse, C.; Cheng, J.; Chau, V.; Sulpizi, M.; Vandevondele, J.; Sprik, M. *J. Phys. Chem. Lett.* **2012**, *3*, 3411.

[258] Adriaanse, C.; Sulpizi, M.; VandeVondele, J.; Sprik, M. *J. Am. Chem. Soc.* **2009**, *131*, 6046.

[259] Dash, J.G.; Fu, H.; Wettlaufer, J.S. *Rep. Prog. Phys.* **1995**, *58*, 115.

[260] Petrenko, V.I.; Whitworth, R.W. "*Physics of Ice*", Physics, Oxford University Press, Oxford, **1999**.

[261] Faraday, M. *Proc. Roy. Soc. Lond.* **1860**, *10*, 440.

[262] Wettlaufer, J.S. *Phys. Rev. Lett.* **1999**, *82*, 2516.

[263] McNeill, V.F.; Loerting, T.; Geiger, F.M.; Trout, B.L.; Molina, M.J. *PNAS* **2006**, *103*, 9422.

[264] McNeill, V.F.; Geiger, F.M.; Loerting, T.; Trout, B.L.; Molina, L.T.; Molina, M.J. *J. Phys. Chem. A* **2007**, *111*, 6274.

[265] Huthwelker, T; Ammann, M.; Peter, T. *Chem. Rev.* **2006**, *106*, 1375.

[266] Bluhm, H.; Ogletree, D.F.; Fadley, Ch.; Hussain, Z.; Salmeron, M. *J. Phys.: Condens. Matter* **2002**, *14*, L227.

[267] Dosch, H.; Lied, A.; Bilgram, J.H. *Surf. Sci.* **1996**, *366*, 43.

[268] Dosch, H.; Lied, A.; Bilgram, J.H. *Surf. Sci.* **1995**, *327*, 145.

[269] Henson, B.F.; Voss, L.F.; Wilson, K.R.; Robinson, J.M. *J. Chem. Phys.* **2005**, *123*, 144707.

[270] Limmer, D.T.; Chandler, D. *J. Chem. Phys.* **2014**, *141*, 18C505.

[271] Kroes, G.J. *Surf. Sci.* **1992**, *275*, 365.

[272] Furukawa, Y.; Nada, H. *J. Phys. Chem. B* **1997**, *101*, 6167.

[273] Nada, H.; Furukawa, Y. *Appl. Surf. Sci.* **1997**, *121*, 445.

[274] Carignano, M.A.; Shepson, P.B.; Szleifer, I. *Mol. Phys.* **2005**, *103*, 2957.

[275] Ikeda-Fukazawa, T.; Kawamura, K. *J. Chem. Phys.* **2004**, *120*, 1395.

[276] Conde, M.M.; Vega, C.; Patrykiejew, A. *J. Chem. Phys.* **2008**, *129*, 014702.

[277] Watkins, M. ; Pan, D.; Wang, E.G.; Michaelides, A.; VandeVondele, J.; Slater, B. *Nature Mater.* **2011**, *10*, 794.

[278] Bishop, C.L.; Pan, D.; Liu, L.M.; Tribello, G.A.; Michaelides, A.; Wang E.G.; Slater, B. *Faraday Discuss.* **2009**, *141*, 277.

[279] Pan, D.; Liu, L.-M.; Tribello, G.A.; Slater, B.; Michaelides, A.; Wang, E. *Phys. Rev. Lett.* **2008**, *101*, 155703.

[280] Pan, D.; Liu, L.-M.; Slater, B.; Michaelides A.; Wang, E. *ACS Nano* **2011**, *5*, 4562.

[281] Pan, D.; Liu, L.-M.; Tribello, G.A.; Slater, B.; Michaelides, A.; Wang, E. *J. Phys.: Condensed Matter* **2010**, *22*, 074209.

[282] Buch, V.; Groenzin, H.; Li, I.; Shultz, M. J.; Tosatti, E. *PNAS* **2008**, *105*, 5969.

[283] Sun, Z.; Pan, D.; Xu, L.; Wang, E. *PNAS* 109, 13177–13181

[284] Krepelová, A.; Newberg, J.T.; Huthwelker, T.; Bluhm, H.; Ammann, M. *Phys. Chem. Chem. Phys.* **2010**, *12*, 8870.

[285] Smith, J.W.; Lam, R.K.; Shih, O.; Rizzuto, A.M.; Prendergast, D.; Saykally, R. J. *J. Chem. Phys.* **2015**, *143*, 084503.

[286] Starr, D.E., Pan, D.; Newberg, J.T.; Ammann, M.; Wang, E.G.; Michaelidis, A.; Bluhm, H. *Phys. Chem. Chem. Phys.* **2011**, *13*, 19988.

[287] Krepelová, A.; Bartels-Rausch, Th.; Brown, M.A.; Bluhm, H.; Ammann, M. *J. Phys. Chem. A* **2013**, *117*, 401.

[288] Newberg, J.T.; Bluhm, H. *Phys. Chem. Chem. Phys.* **2015**, *17*, 23554.